Shale Anisotropy In Situ and in the Lab

or

Serendipity in the quest for C13

Douglas Miller*

MIT FISH Seminar

November 4, 2011

* Formerly Schlumberger, Cambridge MA; currently MIT EAPS and Miller Applied Science, LLC

Serendipity

The faculty of finding valuable or agreeable things not sought for

Shale From Wikipedia, the free encyclopedia

Shale is a fine-grained, clastic sedimentary rock composed of mud that is a **mix of flakes of clay minerals and tiny fragments (silt-sized particles) of other minerals, especially quartz and calcite**.
…
Shale typically exhibits varying degrees of fissility breaking into thin layers, often splintery and usually parallel to the otherwise indistinguishable bedding plane because of parallel orientation of clay mineral flakes.[1] Non-fissile rocks of similar composition but made of particles smaller than 0.06 mm are described as mudstones (1/3 to 2/3 silt particles) or claystone (less than 1/3 silt). Rocks with similar particle sizes but with less clay (greater than 2/3 silt) and therefore grittier are siltstones.[1] Shale is the most common sedimentary rock.[2] …

Clays are the major constituent of shales and other mudrocks. The clay minerals represented are largely kaolinite, montmorillonite and illite. Clay minerals of Late Tertiary mudstones are expandable smectites whereas in older rocks especially in mid to early Paleozoic shales illites predominate. The transformation of smectite to illite produces silica, sodium, calcium, magnesium, iron and water. These released elements form authigenic quartz, chert, calcite, dolomite, ankerite, hematite and albite, all trace to minor (except quartz) minerals found in shales and other mudrocks.[1]

Shales and mudrocks contain roughly 95 percent of the organic matter in all sedimentary rocks. However, this amounts to less than one percent by mass in an average shale. …

Shale Morphology

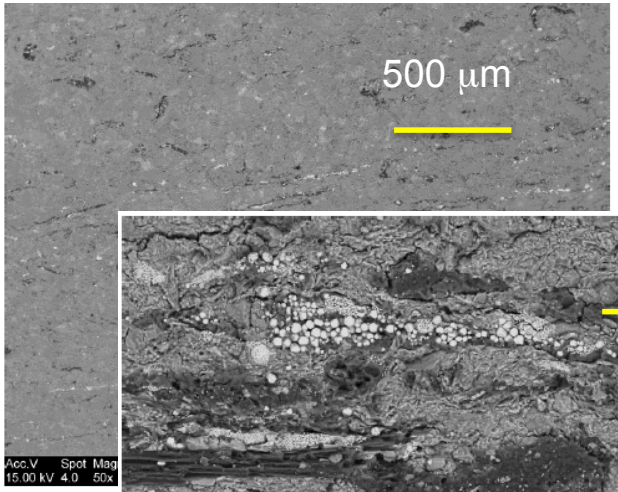

Visually homogeneous

Inclusions of organic matter (dark)
and pyrite (white) reveal bedding plane

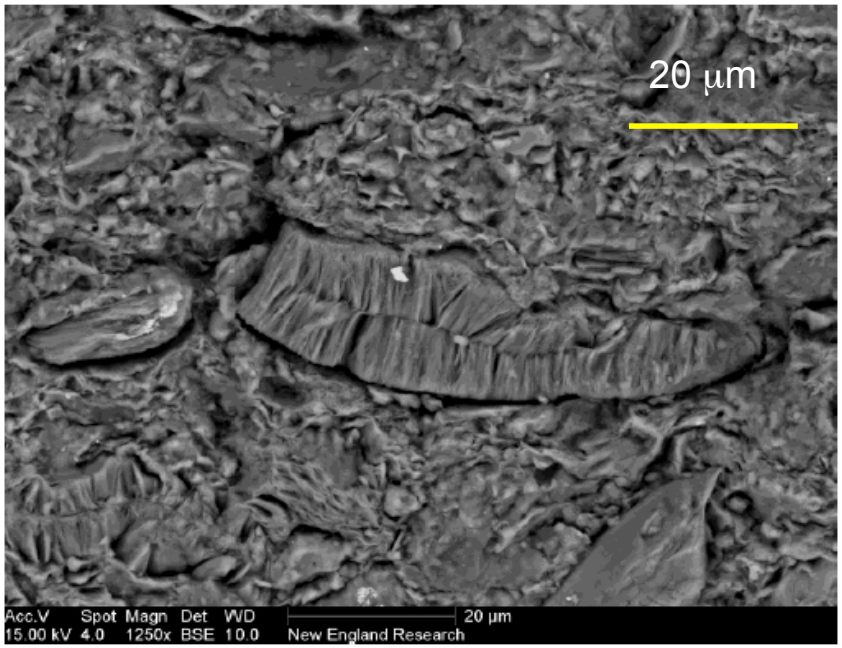

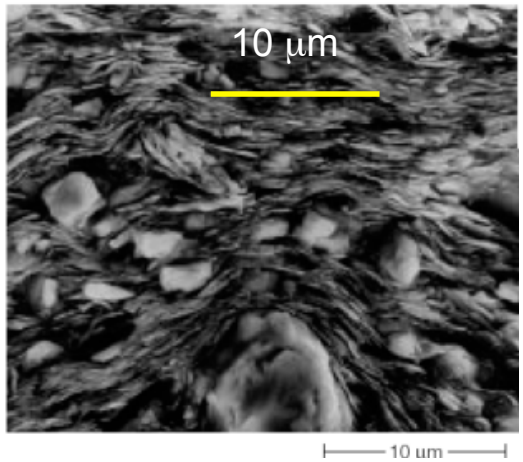

A marine shale with evident granular inclusions

High volume fraction of clay minerals with few detrital grains. Interparticle Porosity is now visible. Evidence of mechanical compaction but no cementation

Estimates of Elastic Moduli

0) Jones & Wang 1981, Greenhorn Shale

c_{ij}	(kbar)
c_{11}	343 ± 14
c_{33}	227 ± 9
c_{44}	54 ± 8
c_{66}	106 ± 16
c_{13}	107 ± 54

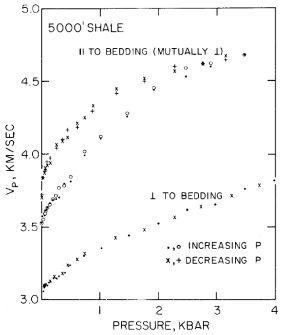

1) Miller, Leaney, Boreland.,1994, Petronas Shale

$A_{11} = 6.99 \pm 0.21$ (km²/sec²)

$A_{33} = 5.53 \pm 0.17$

$A_{qp} = 5.36 \pm 0.16$

$A_{55} = 0.91 \pm 0.05$

$A_{13} = 2.64 \pm 0.26.$

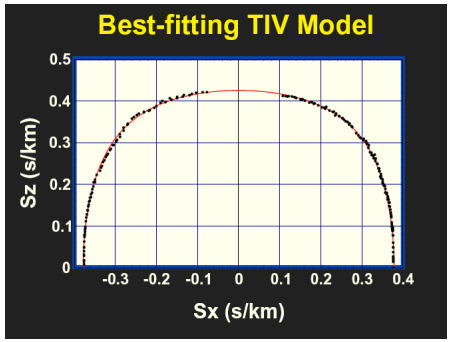

- Note the error estimates for C13
- Note that examples (1) and (2) are made *in situ* and each fits hundreds of data points with a single set of TI parameters
- Today's main objective: Explain (1) and (2)

2) Miller, Horne, Walsh,2011, Gas Shale

Modulus	C_{11}	C_{13}	C_{33}	C_{55}	C_{66}
raw	57.0	16.4	29.0	10.4	19.3
Corrected (GPa)	58.1 ±2.5	16.6 ±1.5	29.6 ±2.0	10.6 ±0.3	19.7 ±0.7

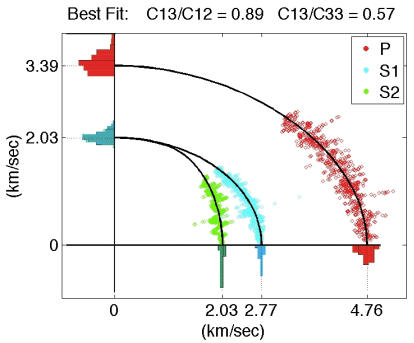

Estimates of Elastic Moduli

1) Miller, Leaney, Boreland.,1994, Petronas Shale

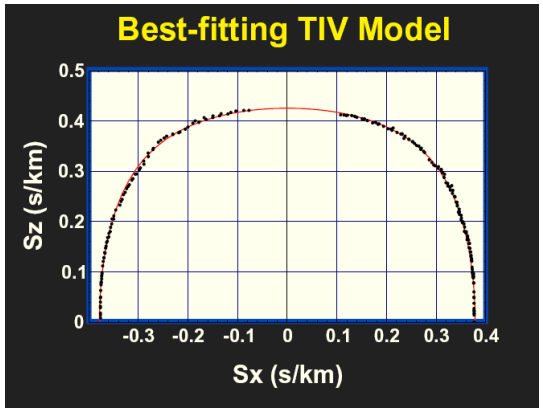

2) Miller, Horne, Walsh,2011, Gas Shale

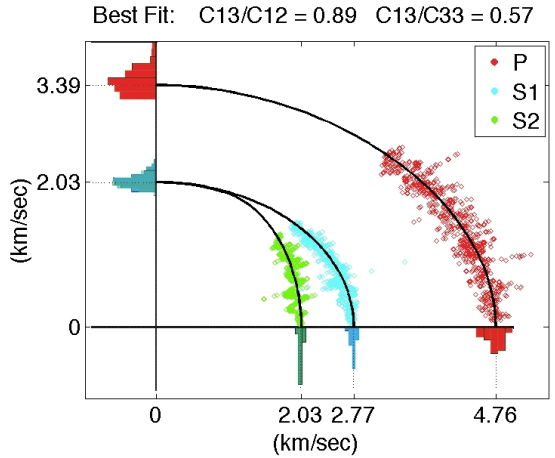

- In each case so-called “data points” are fit by a curve dependent upon TI elastic parameters and reported error estimates are related to rms misfit

- To be clarified:
  - What is path from recorded waveforms to “data point”
  - Why are seismic data points fit by a “phase slowness” curve while sonic data points are fit by a “group velocity” curve?

Today's Discussion

- Some background on anisotropy:
  - Phase & group vectors
- The Borehole Seismic Example
- The Borehole Sonic Example
  - synthetic data & associated processing
  - field data
- A Fresh Can of Worms

for more details: http://www.mit.edu/~demiller

Hooke's Law

- **isotropic**

$$\begin{bmatrix} \sigma_{11} \\ \sigma_{22} \\ \sigma_{33} \\ \sigma_{12} \\ \sigma_{13} \\ \sigma_{23} \end{bmatrix} = \begin{bmatrix} \lambda+2\mu & \lambda & \lambda & & & \\ \lambda & \lambda+2\mu & \lambda & & & \\ \lambda & \lambda & \lambda+2\mu & & & \\ & & & \mu & & \\ & & & & \mu & \\ & & & & & \mu \end{bmatrix} \begin{bmatrix} \epsilon_{11} \\ \epsilon_{22} \\ \epsilon_{33} \\ \epsilon_{12} \\ \epsilon_{13} \\ \epsilon_{23} \end{bmatrix}$$

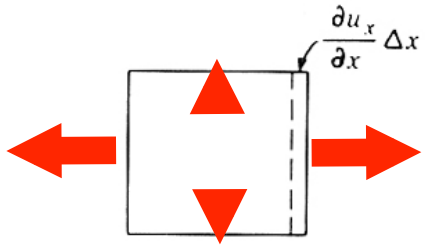

(b) Simple extension

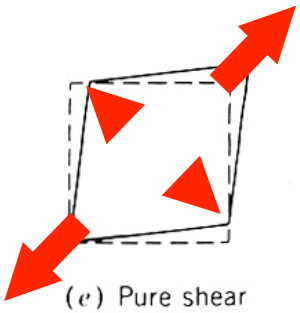

(e) Pure shear

To achieve a unit of pure longitudinal strain along the 1-axis:

- Pull *left-right* with traction $\lambda+2\mu$
- Pull *up-down* with traction λ

To achieve a unit of pure shear strain:

- Squeeze opposite corners with differential traction μ

Hooke's Law

- **TIV - rotational symmetry around 3-axis**

$$\begin{bmatrix} \sigma_{11} \\ \sigma_{22} \\ \sigma_{33} \\ \sigma_{12} \\ \sigma_{13} \\ \sigma_{23} \end{bmatrix} = \begin{bmatrix} c_{1111} & c_{1111}-2c_{1212} & c_{1133} & & & \\ c_{1111}-2c_{1212} & c_{1111} & c_{1133} & & & \\ c_{1133} & c_{1133} & c_{3333} & & & \\ & & & c_{1313} & & \\ & & & & c_{1313} & \\ & & & & & c_{1212} \end{bmatrix} \begin{bmatrix} \epsilon_{11} \\ \epsilon_{22} \\ \epsilon_{33} \\ \epsilon_{12} \\ \epsilon_{13} \\ \epsilon_{23} \end{bmatrix}$$

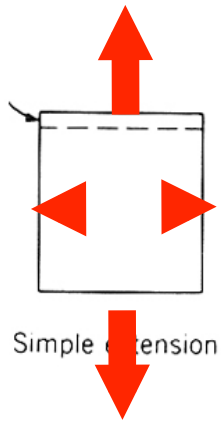

(b) Simple extension

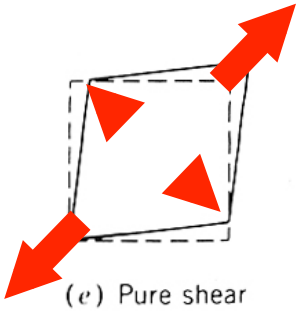

(e) Pure shear

To achieve a unit of pure longitudinal strain along the 3-axis:

- Pull *up-down* with traction c_{3333}
- Pull *left-right, in-out* with traction c_{1133}

To achieve a unit of pure 13 shear strain:

- Apply 13 traction c_{1313}

Hooke's Law: Reduced (Voigt) Notation

- **TIV - rotational symmetry around 3-axis**

$$\begin{bmatrix} \sigma_1 \\ \sigma_2 \\ \sigma_3 \\ \sigma_4 \\ \sigma_5 \\ \sigma_6 \end{bmatrix} = \begin{bmatrix} c_{11} & c_{11}-2c_{66} & c_{13} & & & \\ c_{11}-2c_{66} & c_{11} & c_{13} & & & \\ c_{13} & c_{13} & c_{33} & & & \\ & & & c_{44} & & \\ & & & & c_{44} & \\ & & & & & c_{66} \end{bmatrix} \begin{bmatrix} \epsilon_1 \\ \epsilon_2 \\ \epsilon_3 \\ \epsilon_4 \\ \epsilon_5 \\ \epsilon_6 \end{bmatrix}$$

11	22	33	32 = 23	31 = 13	12 = 21
↓	↓	↓	↓	↓	↓
1	2	3	4	5	6

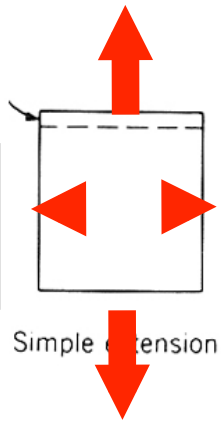

(b) Simple extension

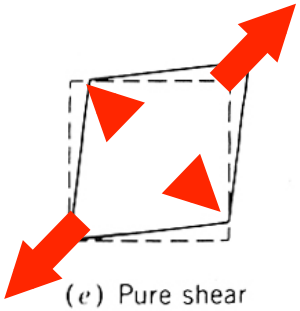

(e) Pure shear

To achieve a unit of pure longitudinal strain along the 3-axis:

- Pull *up-down* with traction c_{33}
- Pull *left-right, in-out* with traction c_{13}

To achieve a unit of pure 13 shear strain:

- Apply 13 traction c_{55}

Alphabet Soup1: Thomsen Parameters

$\alpha = V_{33} = \mathrm{Sqrt}(C_{33}/\rho)$ = vertical P velocity

$\beta = V_{31} = \mathrm{Sqrt}(C_{55}/\rho)$ = vertical S velocity

$\varepsilon = (C_{11} - C_{33})/C_{33}$

$\gamma = (C_{66} - C_{55})/C_{55}$

$\delta = ((C_{13}+C_{55})^2 - (C_{33}-C_{55})^2) / (2\, C_{33}\, (C_{33}-C_{55}))$

- $\delta = 0$ when C13 + 2 C55 = C33 (i.e. when ANNIE 1 condition is true)
- $\delta = \varepsilon$ when qP wavefronts are elliptical

Alphabet Soup2: Engineering Parameters

$$\begin{bmatrix} \epsilon_{11} \\ \epsilon_{22} \\ \epsilon_{33} \\ 2\epsilon_{23} \\ 2\epsilon_{31} \\ 2\epsilon_{12} \end{bmatrix} = \begin{bmatrix} S_{11} & S_{12} & S_{13} & 0 & 0 & 0 \\ S_{21} & S_{22} & S_{23} & 0 & 0 & 0 \\ S_{31} & S_{32} & S_{33} & 0 & 0 & 0 \\ 0 & 0 & 0 & S_{44} & 0 & 0 \\ 0 & 0 & 0 & 0 & S_{55} & 0 \\ 0 & 0 & 0 & 0 & 0 & S_{66} \end{bmatrix} \cdot \begin{bmatrix} \sigma_{11} \\ \sigma_{22} \\ \sigma_{33} \\ \sigma_{23} \\ \sigma_{31} \\ \sigma_{12} \end{bmatrix}$$

where $S_{11} = S_{22}$, $S_{23} = S_{31}$, $S_{44} = S_{55}$, and $S_{66} = 2(S_{11} - S_{12})$

Compliance tensor is inverse of Modulus tensor.

$$S_{11} = S_{22} = \frac{1}{E}, \qquad S_{33} = \frac{1}{E_0}, \qquad S_{12} = -\frac{\nu}{E},$$
$$S_{23} = S_{31} = -\frac{\nu_0}{E_0}, \qquad S_{44} = S_{55} = \frac{1}{\mu_0}, \qquad S_{66} = 2(S_{11} - S_{12}) = \frac{1}{\mu} = \frac{2(1+\nu)}{E}.$$

Amadei et al. 1987: *Gravitational Stresses in Anisotropic Rock Masses*

If the rock mass is transversely isotropic in planes parallel to the ground surface, i.e. plane xy, with the elastic parameters defined in equation (4) and (5), σ_x and σ_y are now equal to

$$\sigma_x = \sigma_y = \sigma_h = \rho g z \frac{\nu_{xz}}{1 - \nu}. \qquad (17)$$

In this equation, ν_{xz} can also be replaced by $\nu' E / E'$. The coefficient K_a is equal to unity. The domain of variation

This asserts $\sigma_{11} = \sigma_{33}$ (C_{13} / C_{33})

F = ma + Hooke's Law =>

Partial Differential Equations for time-stepping solver

Particle velocity:

$$\begin{aligned}
\partial_t v_1 &= \rho^{-1} \left(\partial_1 \sigma_{11} + \partial_2 \sigma_{12} + \partial_3 \sigma_{13} + f_1 \right) \\
\partial_t v_2 &= \rho^{-1} \left(\partial_1 \sigma_{12} + \partial_2 \sigma_{22} + \partial_3 \sigma_{23} + f_2 \right) \\
\partial_t v_3 &= \rho^{-1} \left(\partial_1 \sigma_{13} + \partial_2 \sigma_{23} + \partial_3 \sigma_{33} + f_3 \right).
\end{aligned}$$

F = ma

Stress:

$$\begin{aligned}
\partial_t \sigma_{11} &= c_{11} \partial_1 v_1 + c_{12} \partial_2 v_2 + c_{13} \partial_3 v_3 + c_{15} (\partial_1 v_3 + \partial_3 v_1) \\
\partial_t \sigma_{22} &= c_{12} \partial_1 v_1 + c_{22} \partial_2 v_2 + c_{23} \partial_3 v_3 + c_{25} (\partial_1 v_3 + \partial_3 v_1) \\
\partial_t \sigma_{33} &= c_{13} \partial_1 v_1 + c_{23} \partial_2 v_2 + c_{33} \partial_3 v_3 + c_{35} (\partial_1 v_3 + \partial_3 v_1) \\
\partial_t \sigma_{23} &= c_{44} (\partial_2 v_3 + \partial_3 v_2) + c_{46} (\partial_1 v_2 + \partial_2 v_1) \\
\partial_t \sigma_{13} &= c_{15} \partial_1 v_1 + c_{25} \partial_2 v_2 + c_{35} \partial_3 v_3 + c_{55} (\partial_1 v_3 + \partial_3 v_1) \\
\partial_t \sigma_{12} &= c_{46} (\partial_2 v_3 + \partial_3 v_2) + c_{66} (\partial_1 v_2 + \partial_2 v_1),
\end{aligned}$$

Hooke's Law

where the particle-velocity vector is

$$\mathbf{v} = (v_1, v_2, v_3) = (\partial_t u_1, \partial_t u_2, \partial_t u_3).$$

Cf. Carcione: *Wave Fields in Real Media - Wave Propagation in Anisotropic, Anelastic and Porous Media*

Finite Difference = Time-stepping the PDE

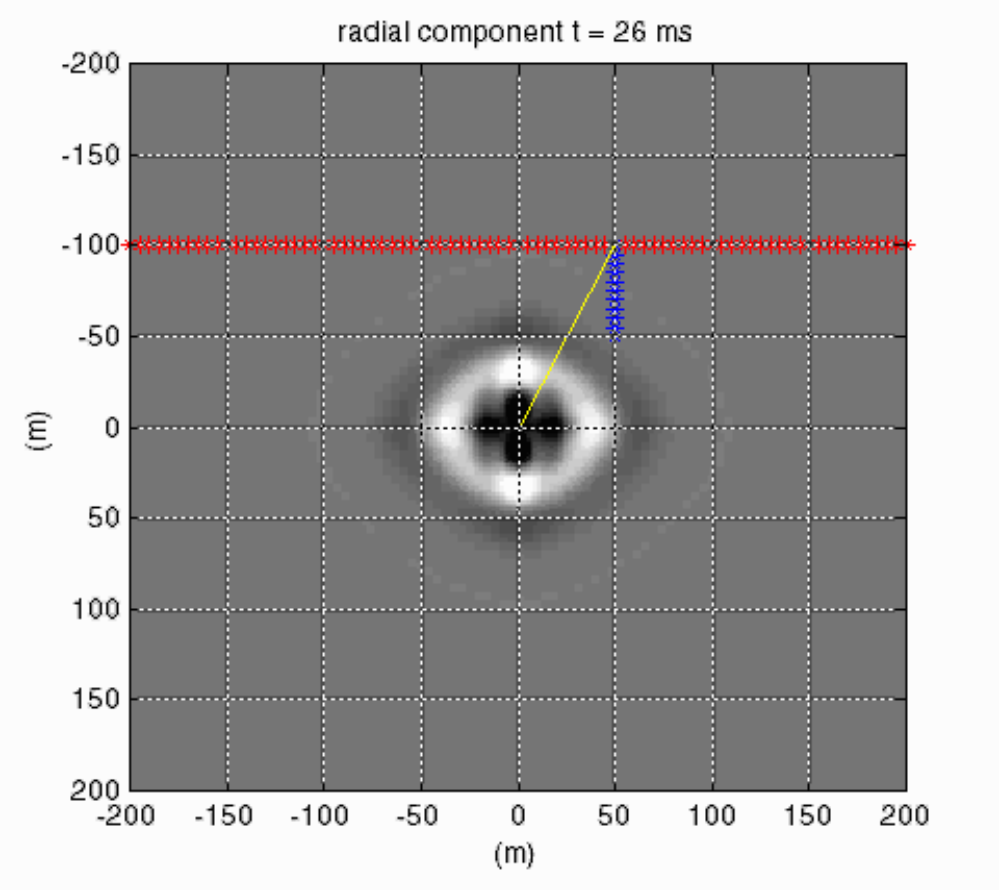

F = ma + Hooke's Law => Spatial Dispersion Analysis

HL + $F = ma$ + $\mathbf{u} = \hat{\mathbf{g}}e^{(i\omega(\mathbf{p}\cdot\mathbf{x}-t))}$ gives the Christoffel (Eigenvalue) Equation:

$$[p_i p_l c_{ijkl} - \rho\delta_{jk}]\hat{g}_k = 0$$

- A solution exists when $Det(matrix) = 0$. This is the **Christoffel Relation** that implicitly defines the phase slowness surface:

$$\mathcal{S} = \{\mathbf{p} : |[p_i p_l c_{ijkl} - \rho\delta_{jk}]| = 0\}$$

-

$$a_{ijkl} = c_{ijkl}/\rho$$

$$A_{11} = a_{xxxx},\ A_{13} = a_{xxzz},\ A_{55} = a_{xzxz},\ \ldots$$

N.B.: Aij have units of velocity^2

F = ma + Hooke's Law =>
Spatial Dispersion Analysis

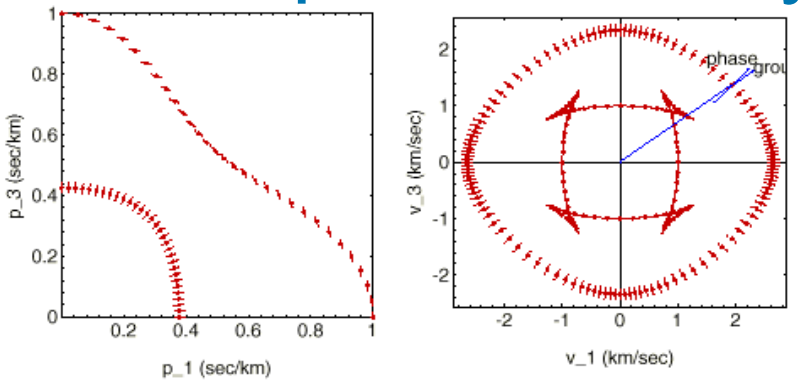

Dispersion Relation:

$$A_{11}A_{55}p_1^4 + A_{33}A_{55}p_3^4 + Ap_1^2p_3^2 - (A_{11} + A_{55})p_1^2 - (A_{33} + A_{55})p_3^2 + 1 = 0$$

$$A = A_{11}A_{33} + A_{55}^2 - (A_{13} + A_{55})^2$$

$$\mathbf{p} \cdot \mathbf{v} = 1$$

Given A_{ij}'s and a phase angle θ, The above equations can be solved for phase vector, **p**, and group vector, **v**, with associated magnitudes (phase slowness, group velocity) and group angle.

Associated eigenvectors are polarizations. These equations are for coupled qP and qSV with polarization in vertical 1-3 plane. SH has a quadratic Dispersion relation with elliptical phase slowness and group velocity curves.

FD gives animations; Christoffel gives annotations

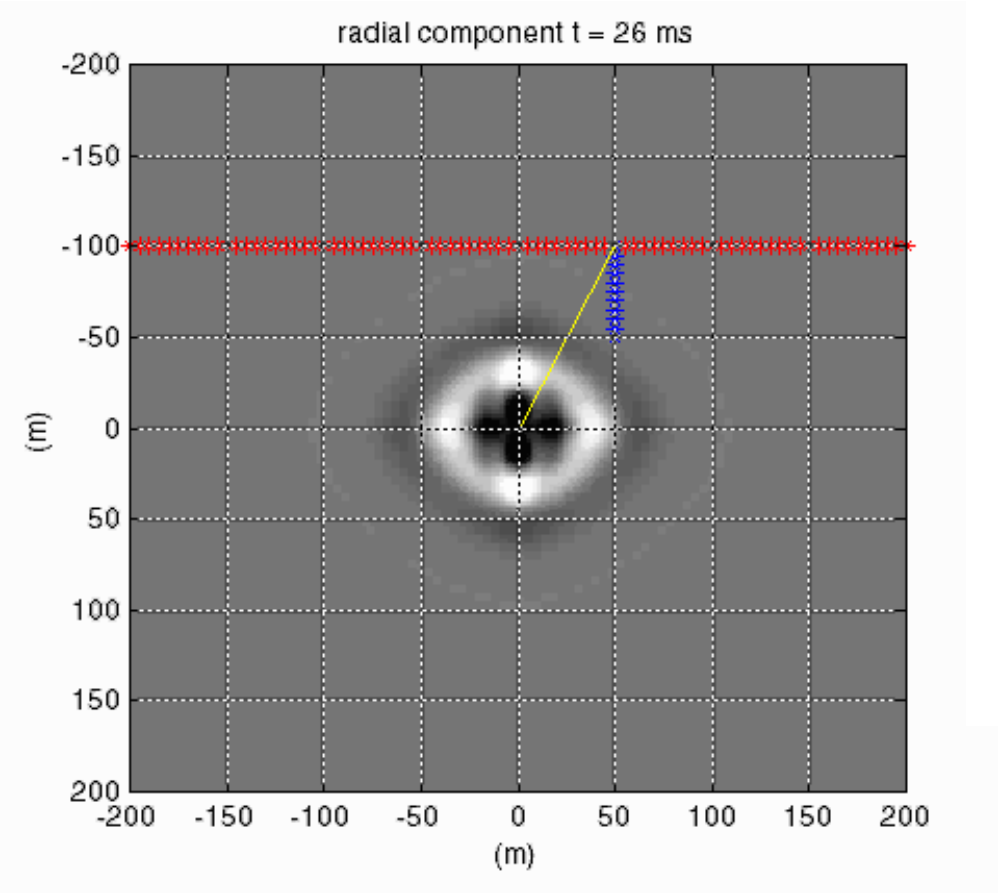

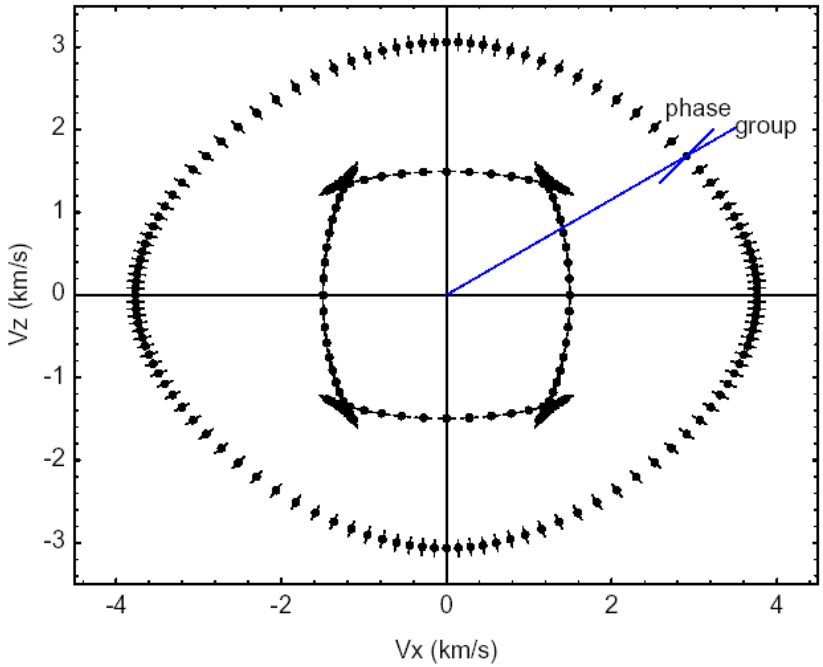

- Group direction points to source
- Phase direction is normal to wavefront

FD gives animations; Christoffel gives annotations

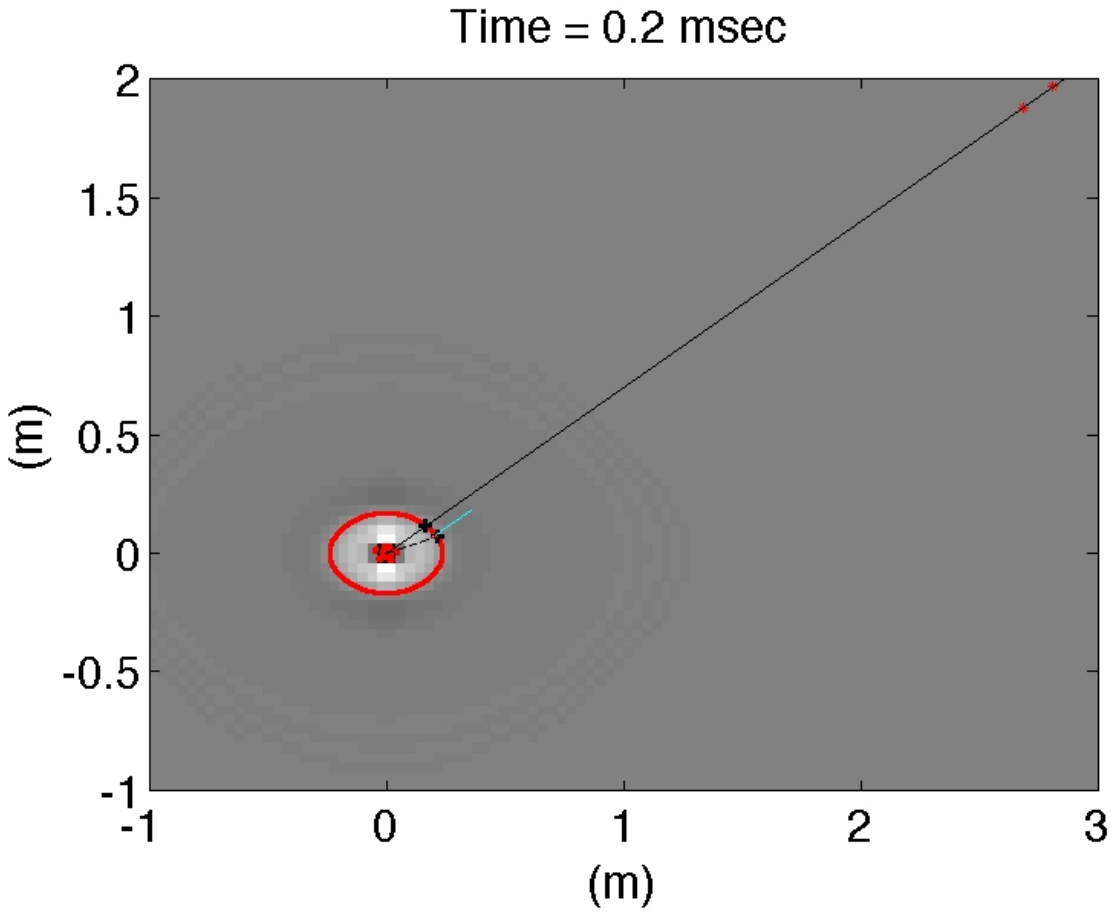

- Wavefront expands without changing shape
- Group direction points to source
- Phase direction is normal to wavefront
- Marked points have 55 degree group and phase angles respectively

Phase and Group

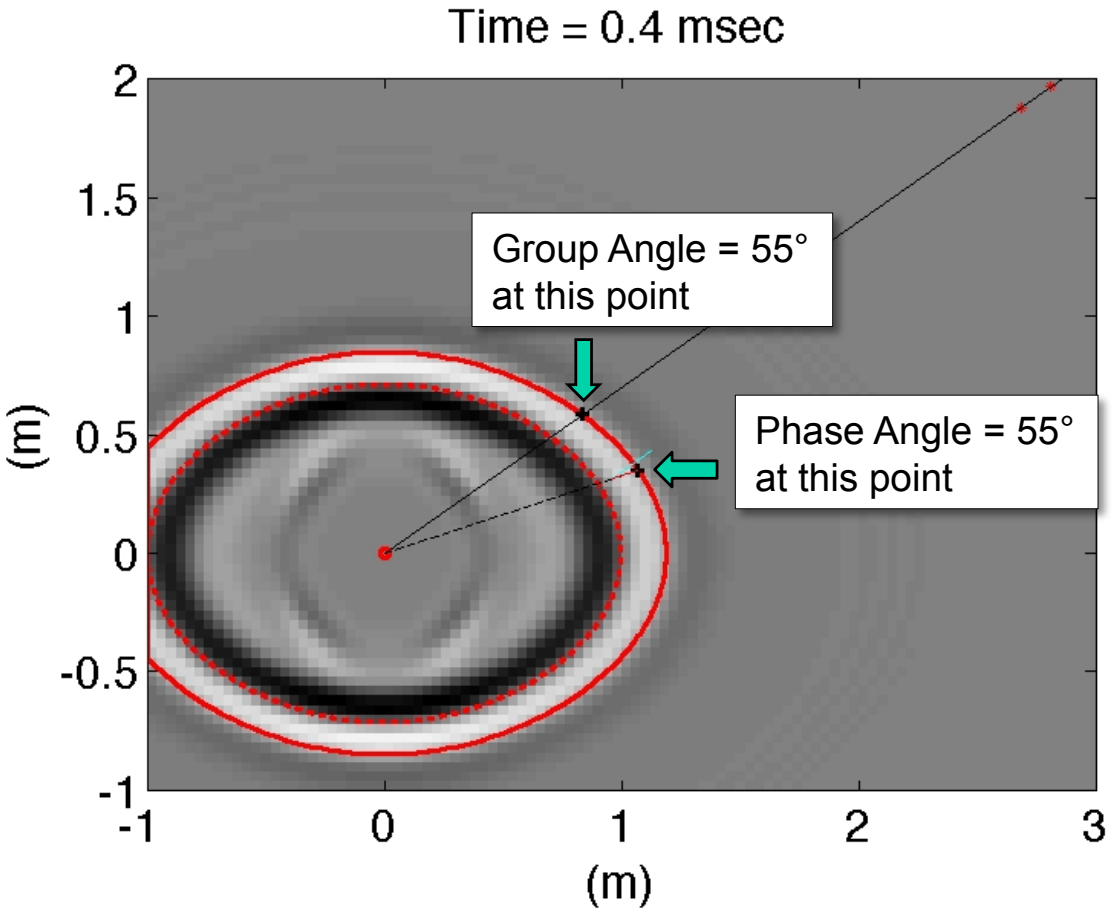

- Wavefront expands without changing shape
- Group direction points to source
- Phase direction is normal to wavefront
- Marked points have 55 degree group and phase angles respectively

Phase and Group

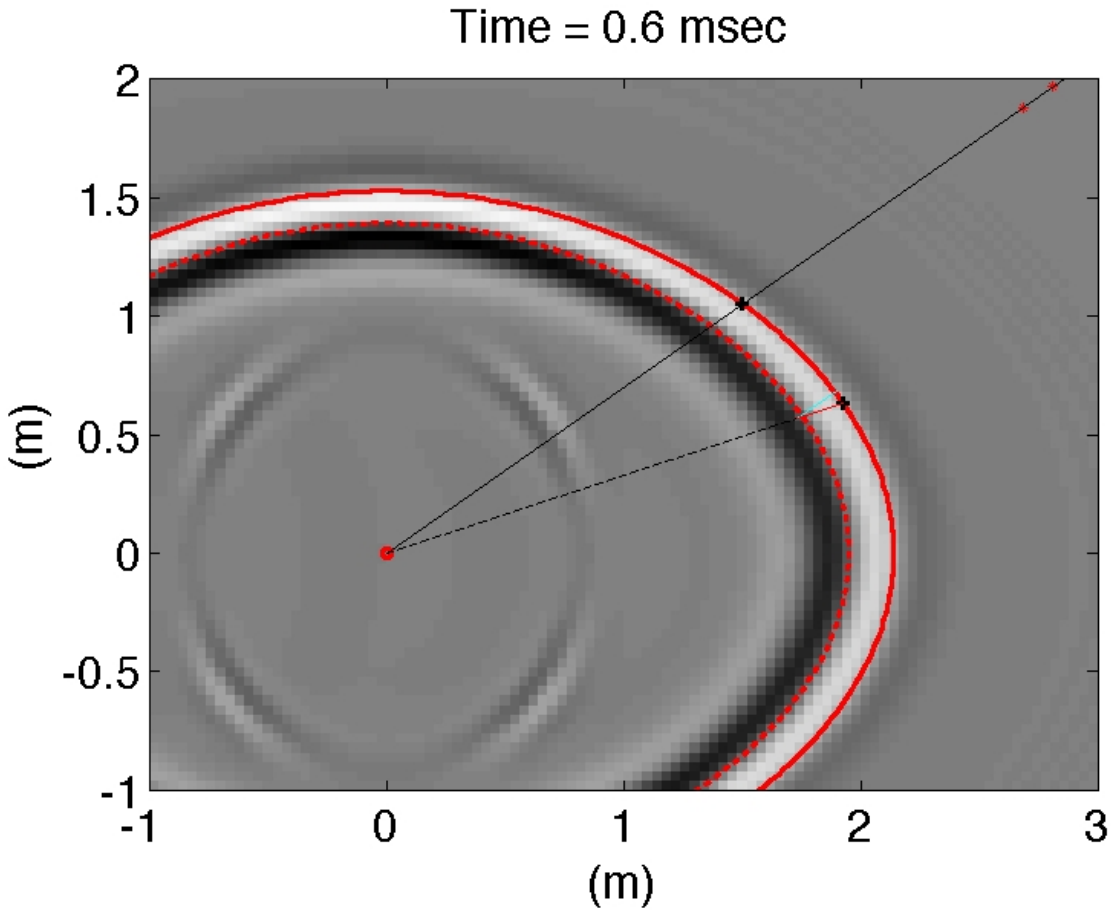

- Wavefront expands without changing shape
- Group direction points to source
- Phase direction is normal to wavefront
- Marked points have 55 degree group and phase angles respectively

FD gives animations; Christoffel gives annotations

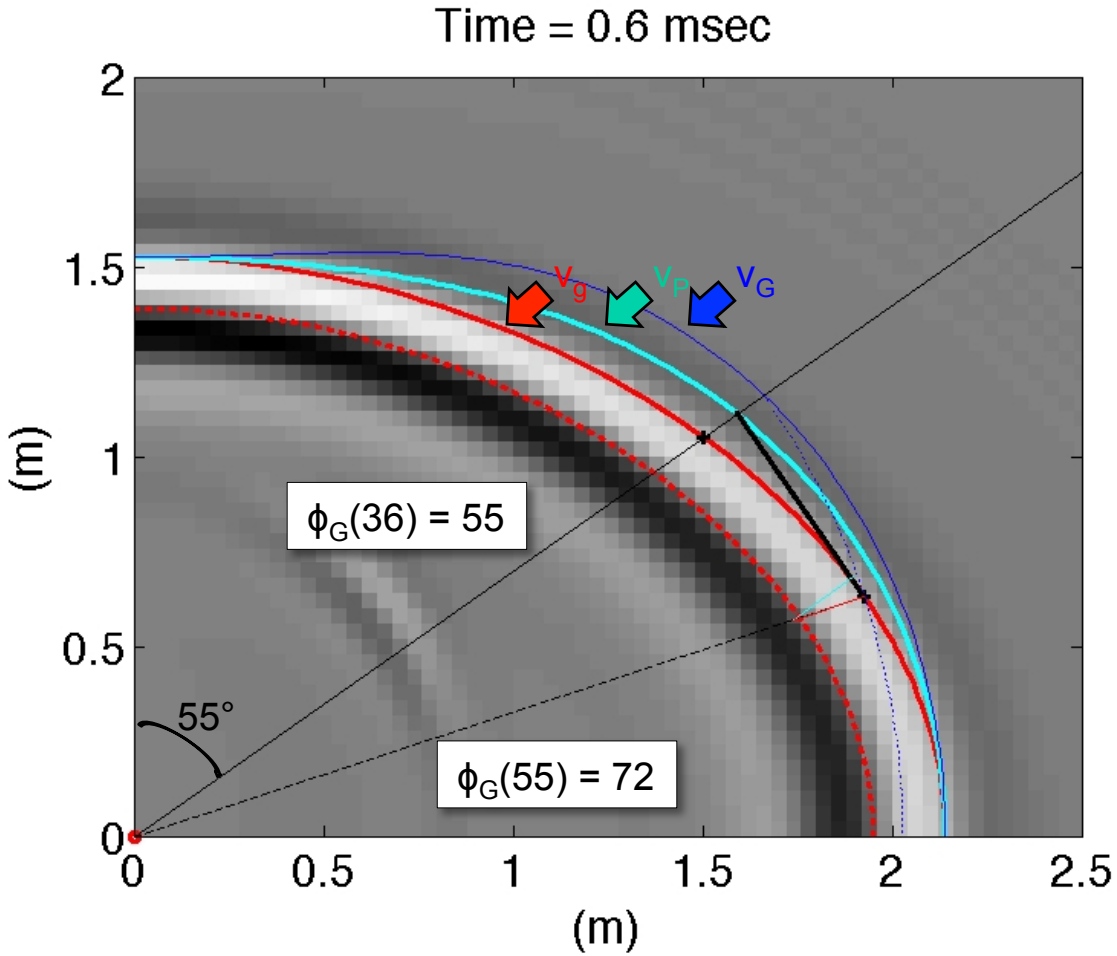

- v_g is **Group velocity(group angle)**
- v_P is **Phase velocity(phase angle)**
- v_G is **Group velocity(phase angle)**

- v_g matches the wavefront

- v_P , v_G and ϕ_G can be computed algebraically from phase angle

- v_g must be interpolated as
  $v_G(\phi_G(\text{phase angle}))$

That's "group velocity at phase angle whose associated group angle is as required"

- For qP and SH modes in TI media, and all ψ,

$$v_G(\psi) \geq v_P(\psi) \geq v_g(\psi)$$

(2^{nd} inequality because phase surface is convex)

Fixed Orthogonal Arrays => Phase Vector

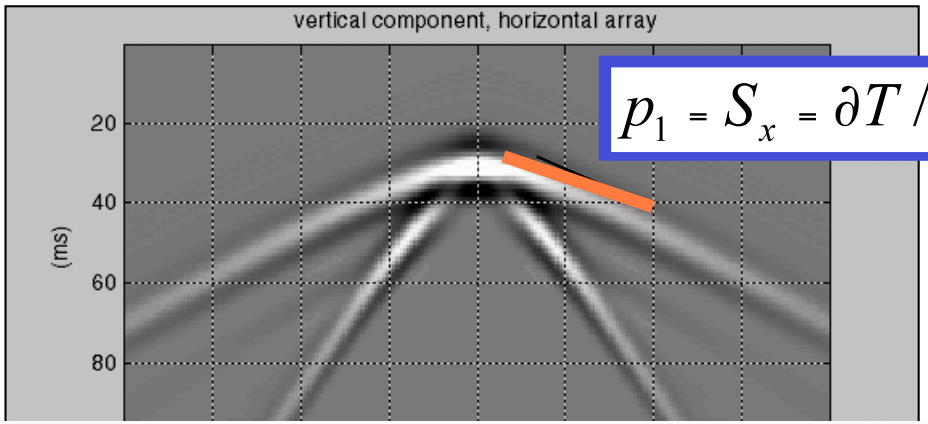

$$p_1 = S_x = \partial T / \partial x$$

Apparent moveout on a horizontal array is the x-component of phase slowness

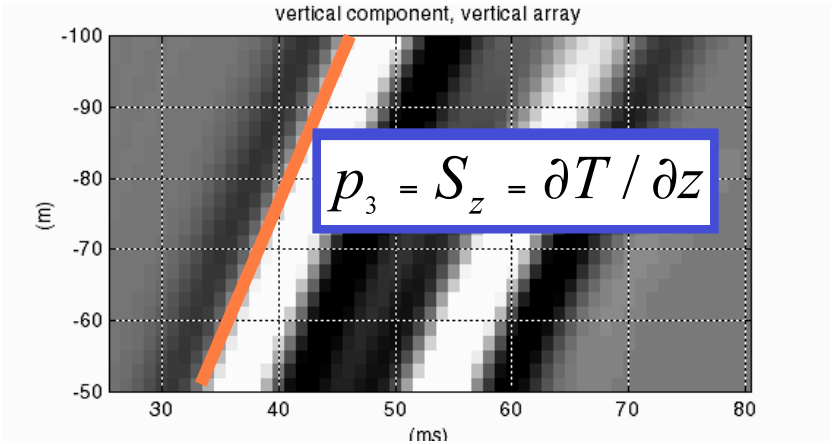

$$p_3 = S_z = \partial T / \partial z$$

Apparent moveout on a vertical array is the z-component of phase slowness

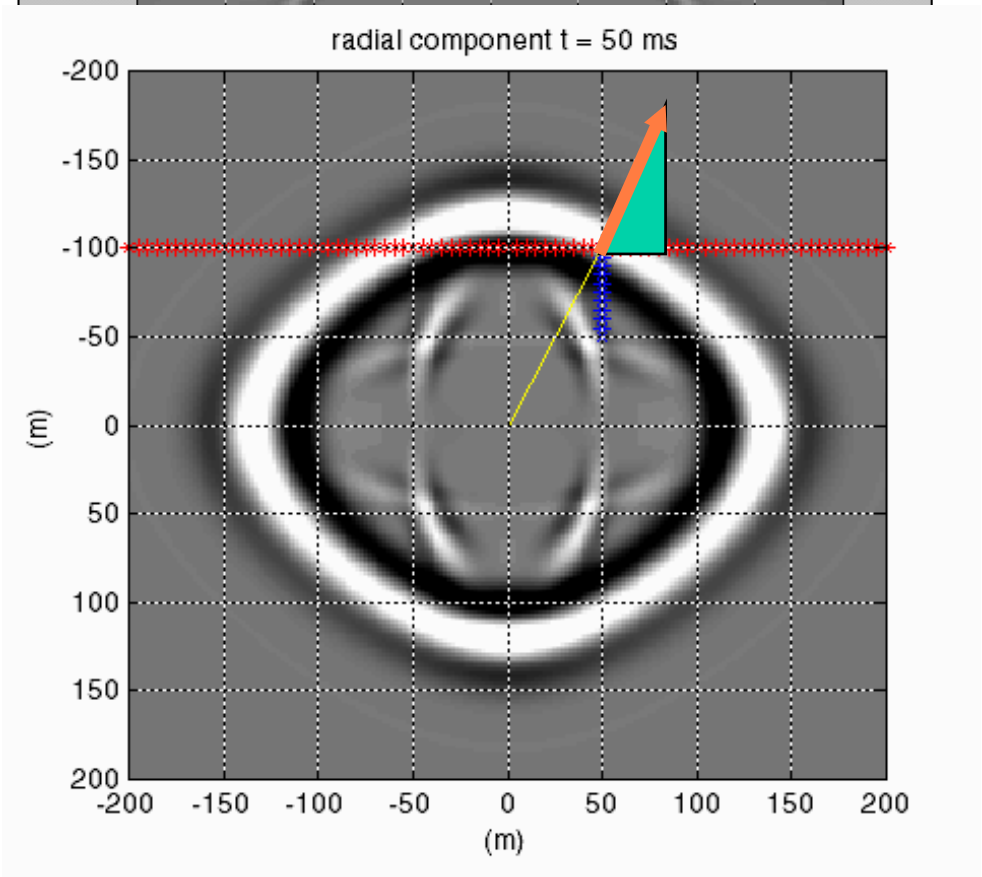

The spatial gradient of the traveltime function is the Phase Slowness Vector

Today's Discussion

- Some background on anisotropy:
  - Phase & group vectors
- The Borehole Seismic Example
- The Borehole Sonic Example
  - synthetic data & associated processing
  - field data
- A Fresh Can of Worms

for more details: http://www.mit.edu/~demiller

How does this look in Walkaway VSP Data?

5129 Sound velocities

AN *IN SITU* ESTIMATION OF ANISOTROPIC ELASTIC MODULI FOR A SUBMARINE SHALE.

Douglas E. Miller (Schlumberger-Doll Research, Old Quarry Road, Ridgefield CT 06977-4108, USA; (email: miller@sdr.slb.com))
Scott Leaney, Bill Borland

Direct arrival times and slownesses from wide aperture walkaway vertical seismic profile data acquired in a layered anisotropic medium can be processed to give a direct estimate of the phase slowness surface associated with the medium at the depth of the receivers. This slowness surface can, in turn, be fit by an estimated transversely isotropic medium with a vertical symmetry axis (a "TIV" medium). While the method requires that the medium between the receivers and the surface be horizontally stratified, no further measurement or knowledge of that medium is required. When applied to data acquired in a compacting shale sequence (here termed the "Petronas shale") encountered by a well in the South China Sea, the method yields an estimated TIV medium that fits the data extremely well over 180 degrees of propagation angles sampled by 201 source positions. The medium is strongly anisotropic. The anisotropy is significantly anelliptic and implies that the quasi-shear mode should be triplicated for off-axis propagation. Estimated density-normalized moduli (in units of km^2/s^2) for the Petronas shale are: $A_{11} = 6.99 \pm .21$; $A_{33} = 5.53 \pm .17$; $A_{55} = .91 \pm .05$; $A_{13} = 2.64 \pm .26$. Densities in the logged zone just below the survey lie in the range between 2200 and 2400 km^3/m^3 with an average value close to 2300 km^3/m^3.

Compaction Process

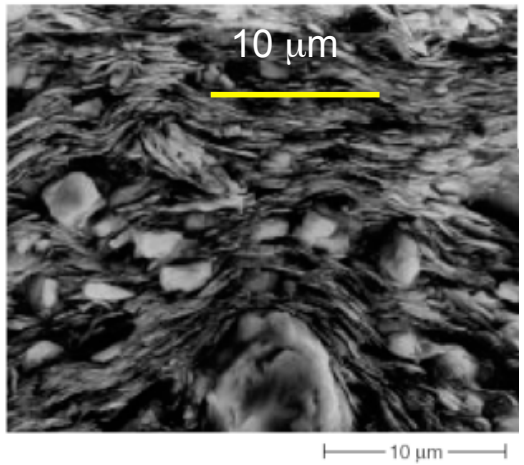

Expectation:

As depth increases

- Porosity decreases so velocity increases
- Order increases so anisotropy increases (up to a point)

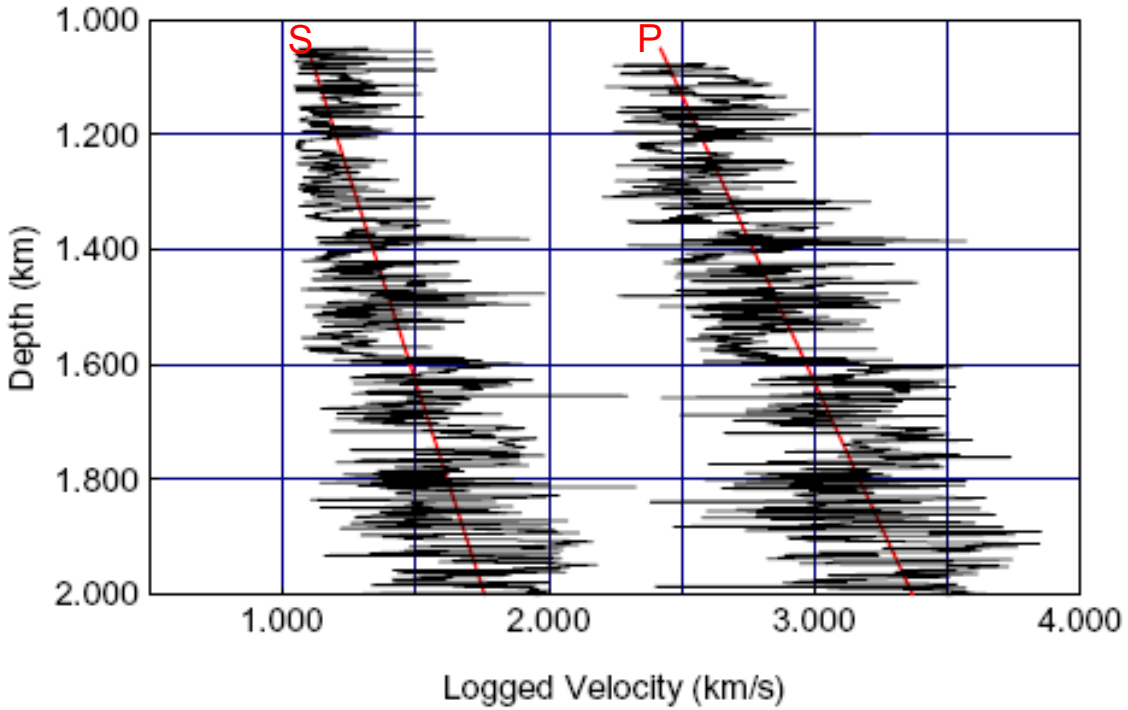

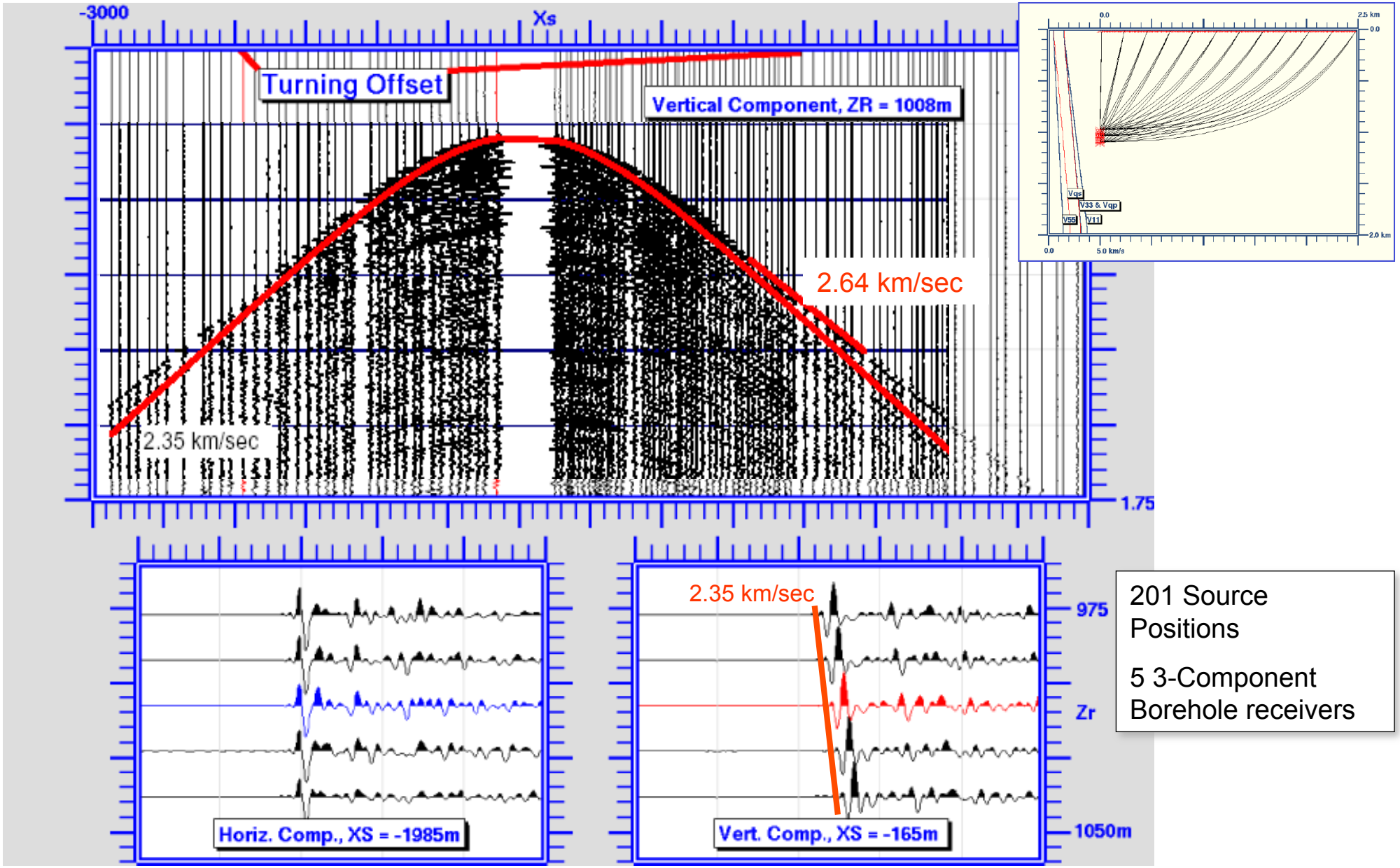

Walkaway VSP Example

White, et al., 1983

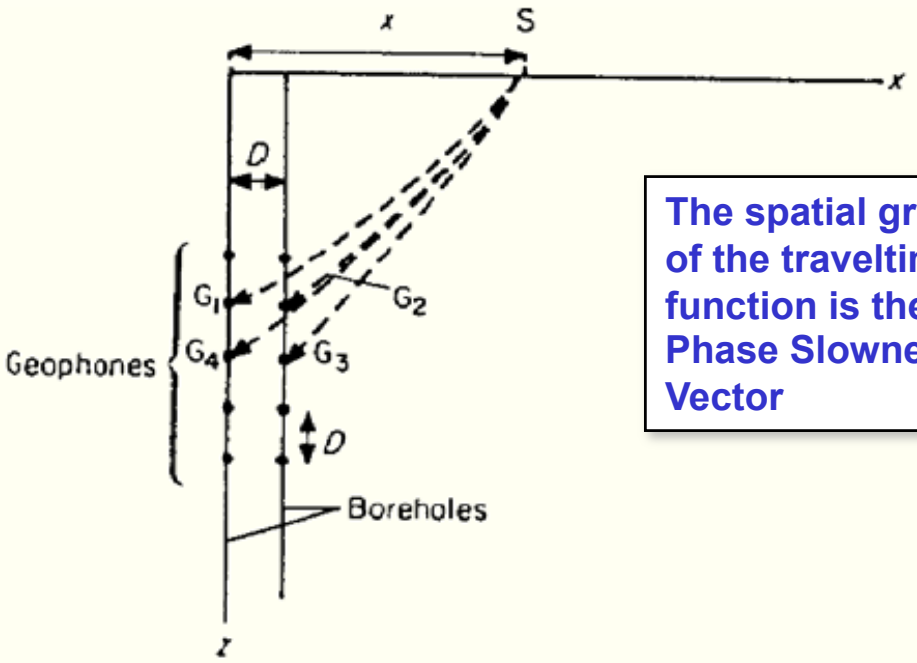

The spatial gradient of the traveltime function is the Phase Slowness Vector

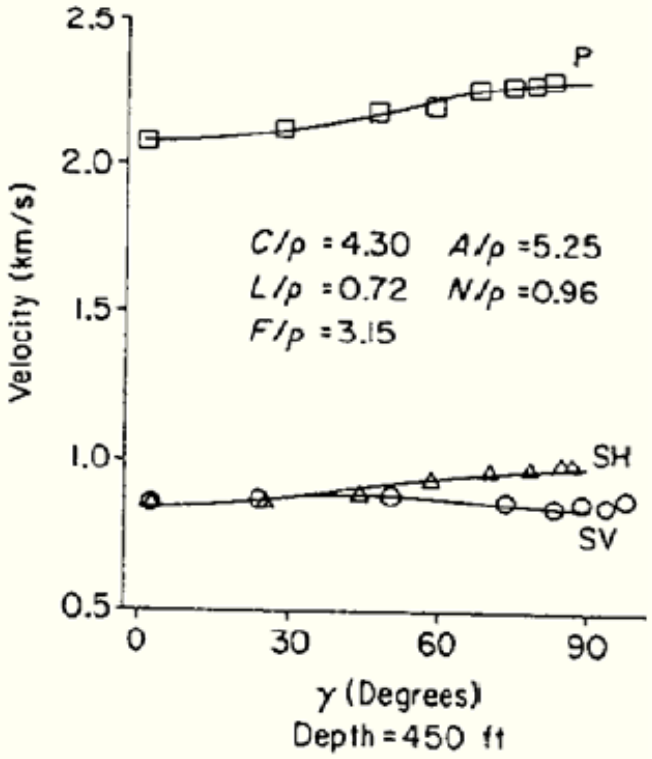

$$\Delta t_h = (t_1 - t_2 + t_4 - t_3)/2,$$

$$\Delta t_v = (t_3 - t_2 + t_4 - t_1)/2.$$

$$V_h = \frac{D}{\Delta t_h}$$

$$V_v = \frac{D}{\Delta t_v}$$

$$V_{PH} = [(1/V_h)^2 + (1/V_v)^2]^{-1/2},$$

$$\gamma = \tan^{-1}[V_v/V_h].$$

Key Observation

In a laterally invariant medium the horizontal component of slowness preserved along the ray and can be measured by estimating dT/dX at the source.

Our single vertical array with many sources is equivalent to a 2D array with a single source.

Meisner, 1961
Wave-front Diagrams

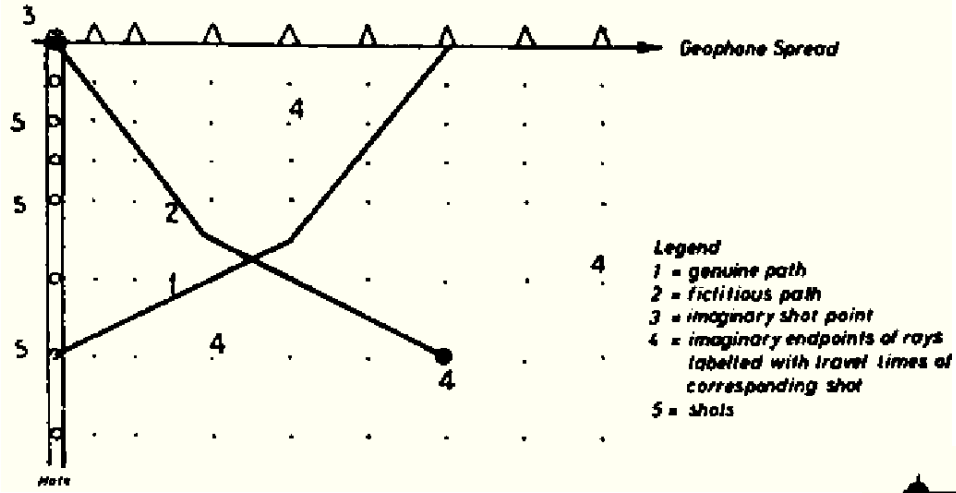

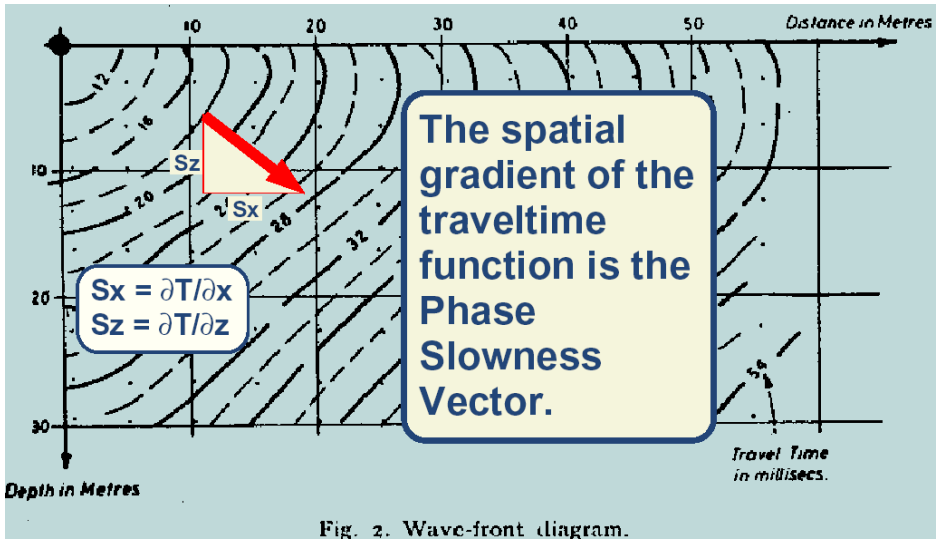

Fig. 2. Wave-front diagram.

J. Gaiser (1992) used this method to estimate phase slownesses which he inverted for TIV parameters.

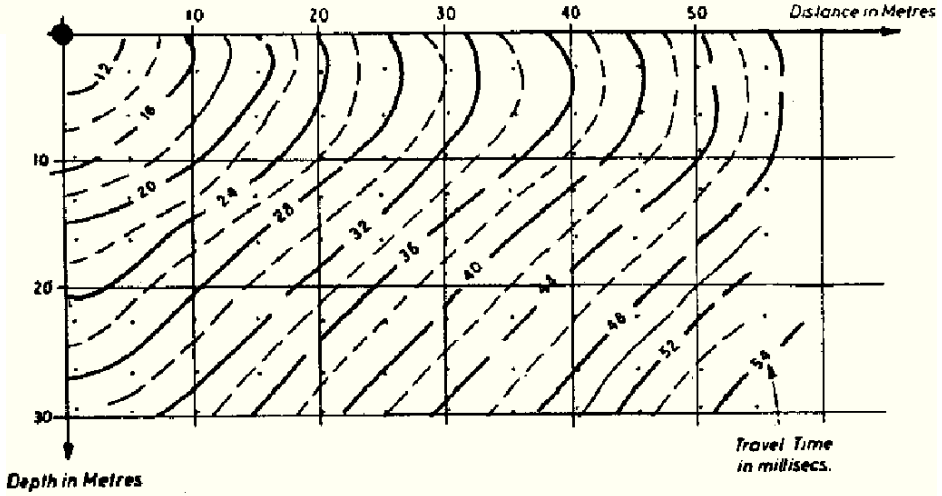

Fig. 2. Wave-front diagram.

Fixed Orthogonal Arrays => Phase Vector

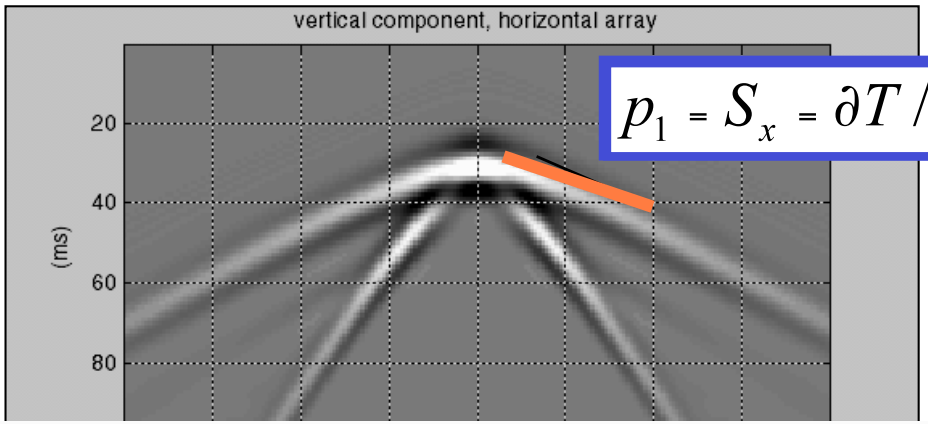

$$p_1 = S_x = \partial T / \partial x$$

Apparent moveout on a horizontal array is the x-component of phase slowness

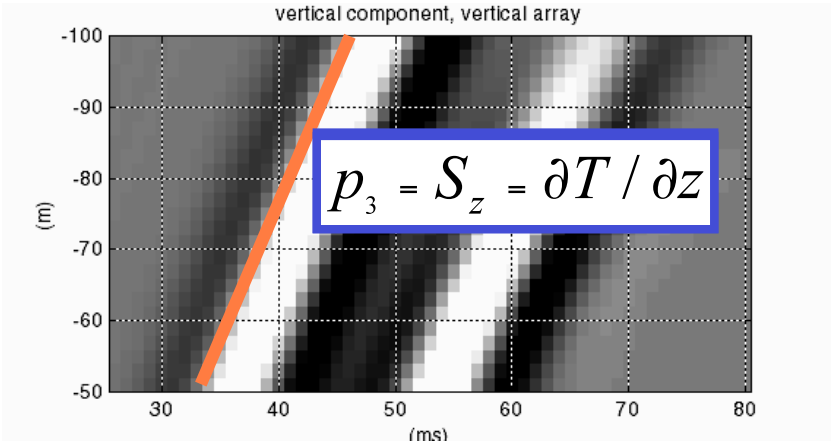

$$p_3 = S_z = \partial T / \partial z$$

Apparent moveout on a vertical array is the z-component of phase slowness

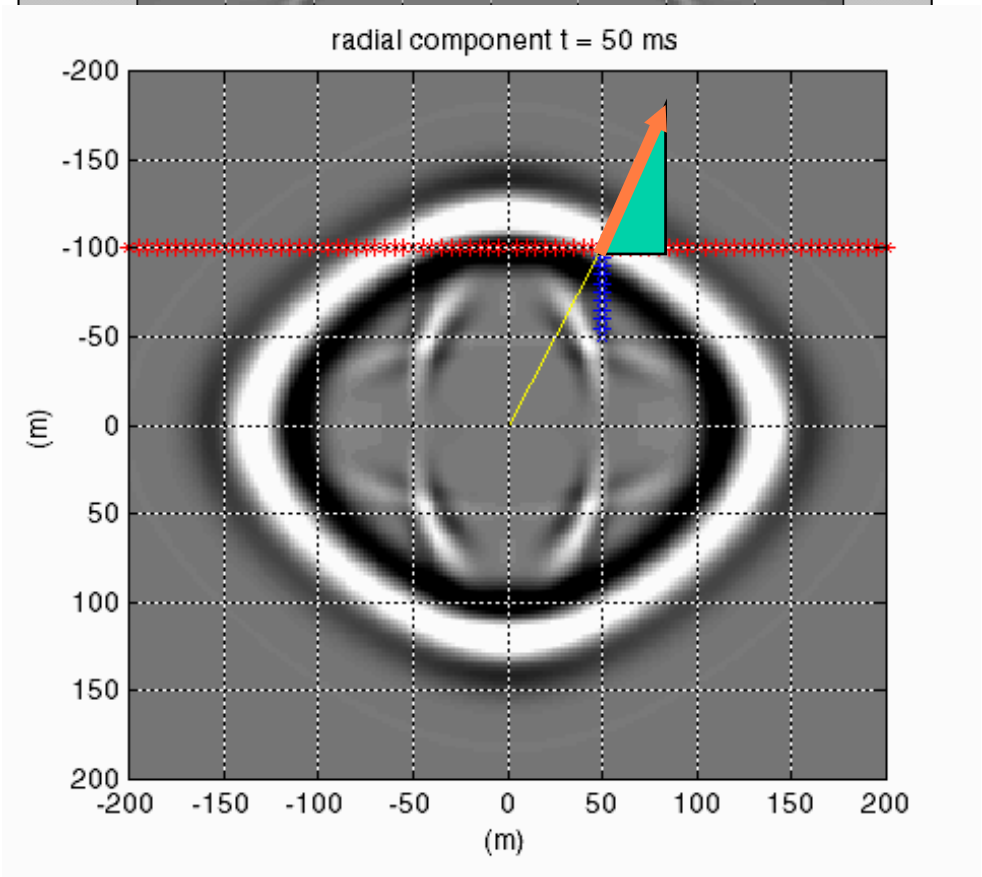

The spatial gradient of the traveltime function is the Phase Slowness Vector

Squared Phase Slowness

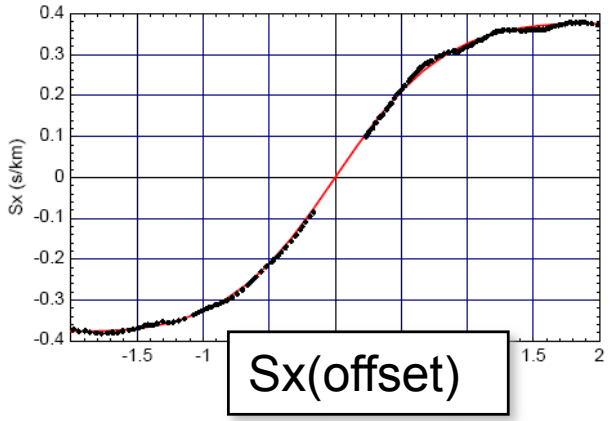

Sx(offset)

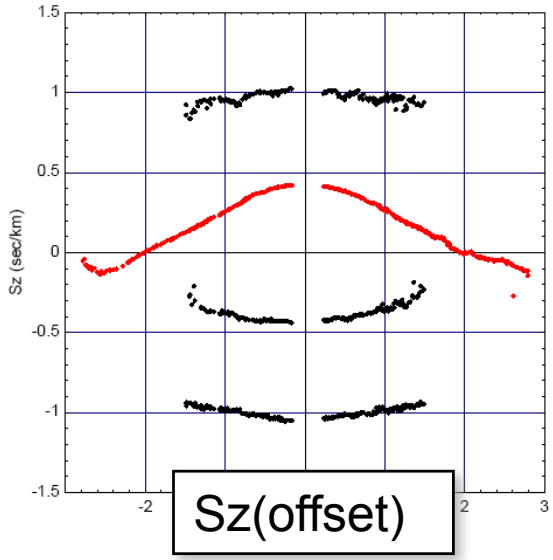

Sz(offset)

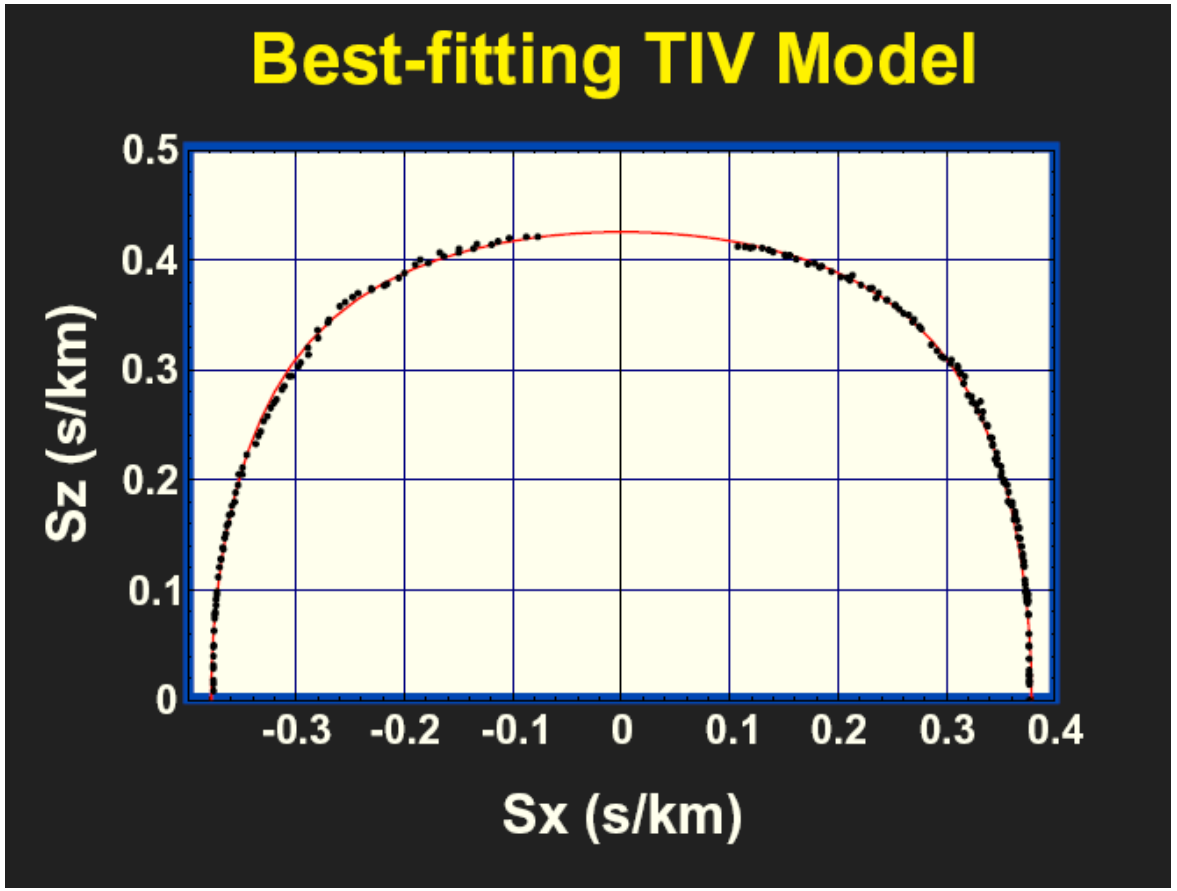

Crossplot of Sx and Sz gives phase slowness

Sx is estimated from common receiver gathers;
Sz is estimated from common shot gathers

Squared Phase Slowness

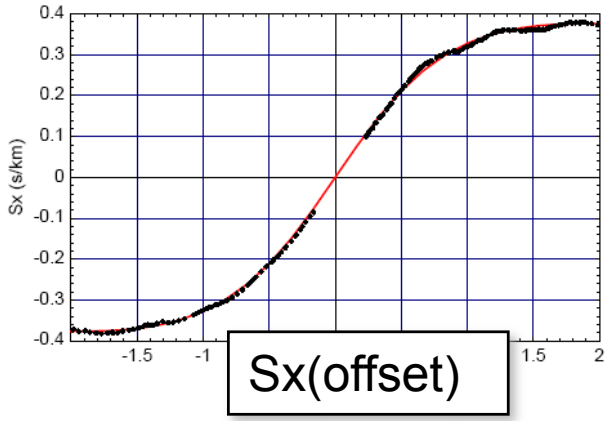

Sx(offset)

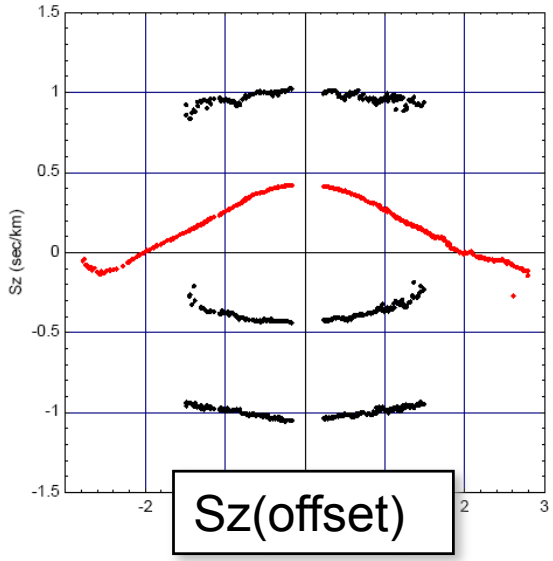

Sz(offset)

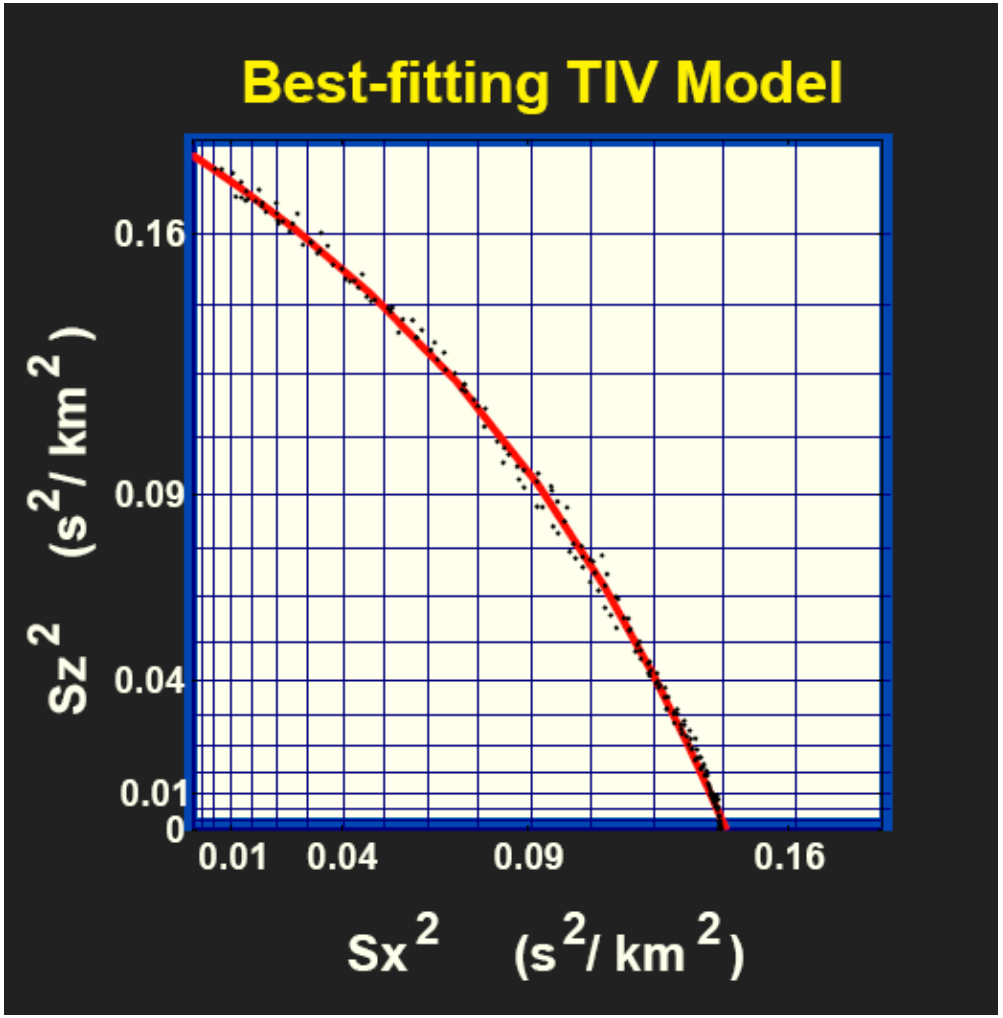

N.B.: Isotropy would require a line at 45^{o}

Remarks about the Model:

- **The isotropic approximation doesn't fit at all**
- **The elliptic approximation fits poorly**
- **The fit is independent of shear modulus used but demands cusp on qSV**
- **With qP only, we can estimate C11, C33, and C13+2 C55**
- **With marine walkaway we get no SH, hence no estimate of C66**

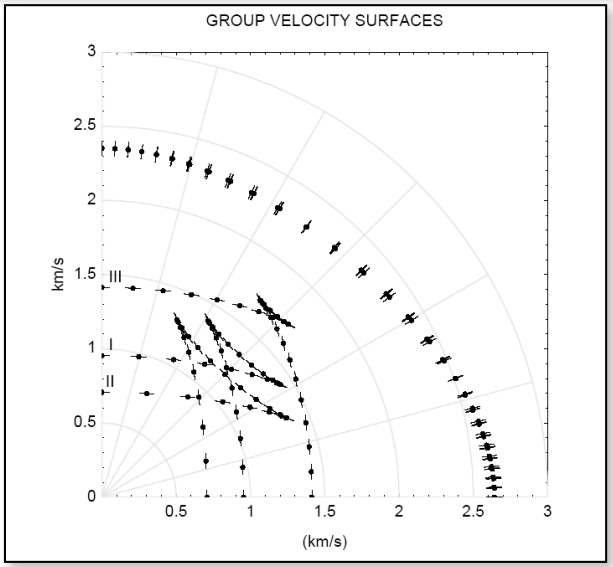

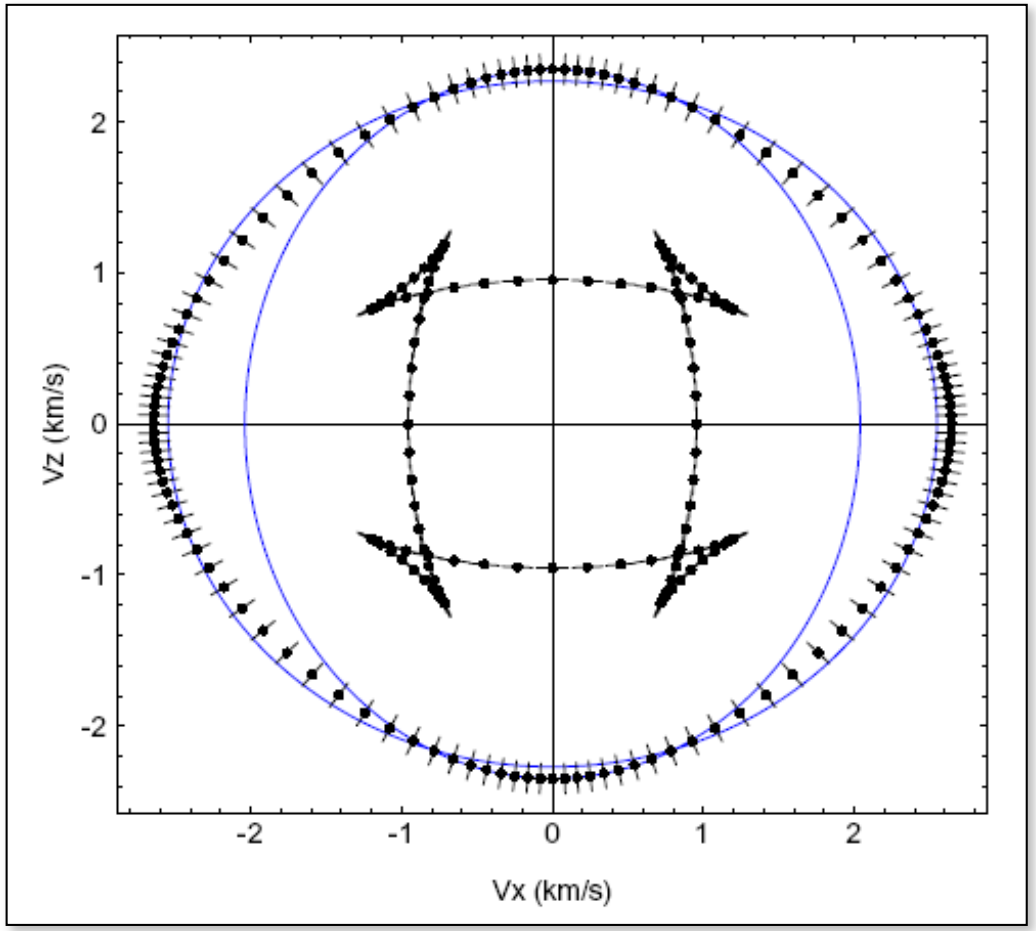

Today's Discussion

- Some background on anisotropy:
  - Phase & group vectors
- The Borehole Seismic Example
- The Borehole Sonic Example
  - synthetic data & associated processing
  - field data
- A Fresh Can of Worms

for more details: http://www.mit.edu/~demiller

How does this look in Sonic Log Data?

Precise Estimation of Elastic Moduli from Sonic Log Data in a Gas Shale Formation

Douglas Miller, Steve Horne, John Walsh3

1st International Workshop in Rock Physics
10 August, 2011

Radial Arrays => Group Vector

- Apparent moveout on a radial array is group slowness at the angle which matches the array inclination

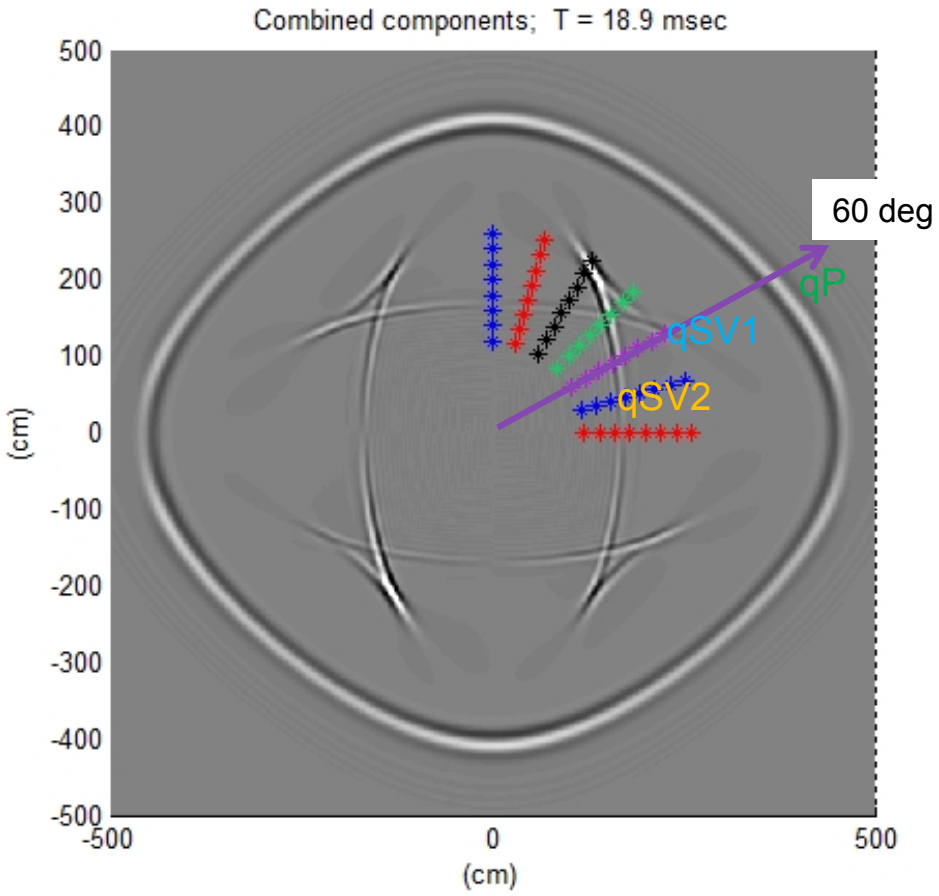

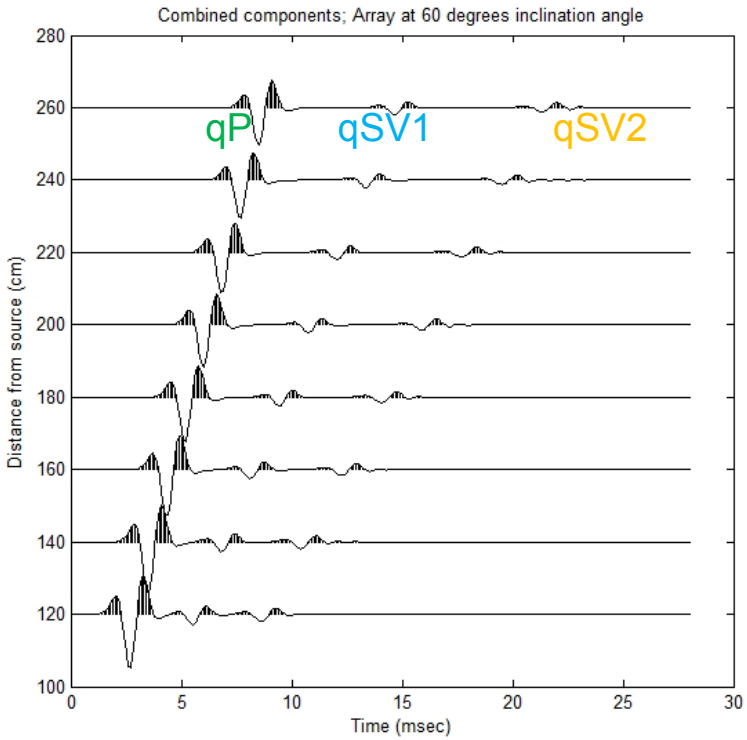

Slowness Time Coherence

- Body wave arrivals are non-dispersive
- STC finds shift that aligns signal
- Slowness values are analytic answer:

Group slowness at phase angle whose group angle is array inclination angle

Given a window function $w(t)$, an array of N waveforms $D(t, r_i)$ as in Figure 9, and a slowness, s, we can form a shifted, muted array

$$D_s(t, r_n) = w(t)D(t + s(r_n - r_1), r_n) \quad (8)$$

and calculate semblance

$$semb(s) = \frac{\sum_t (\sum_n D_s(t, r_n))^2}{N \sum_t \sum_n D_s(t, r_n)^2} \quad (9)$$

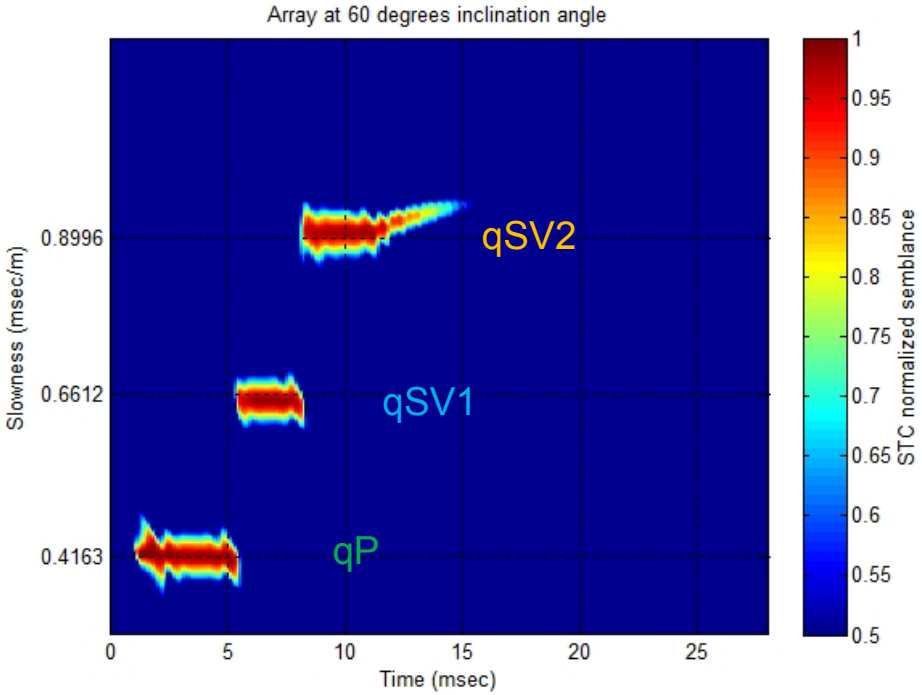

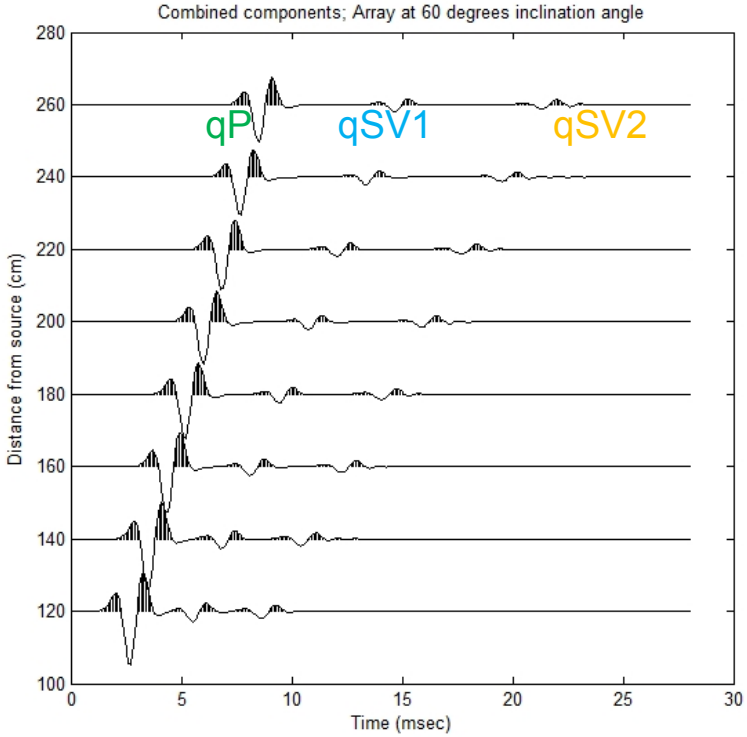

STC for 19 radial arrays

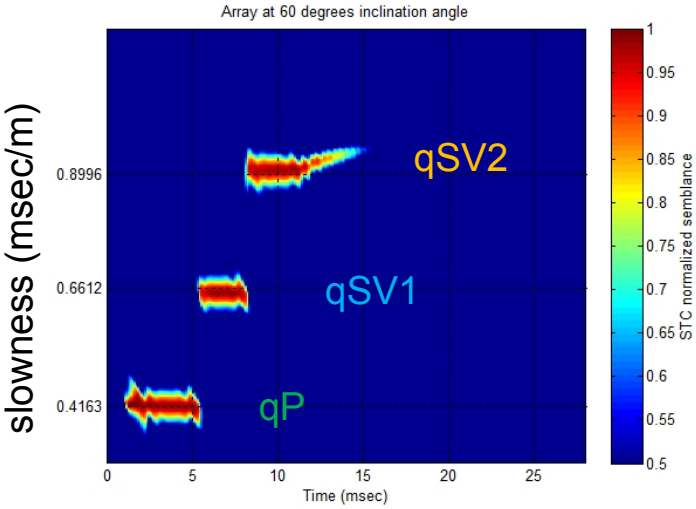

60 deg

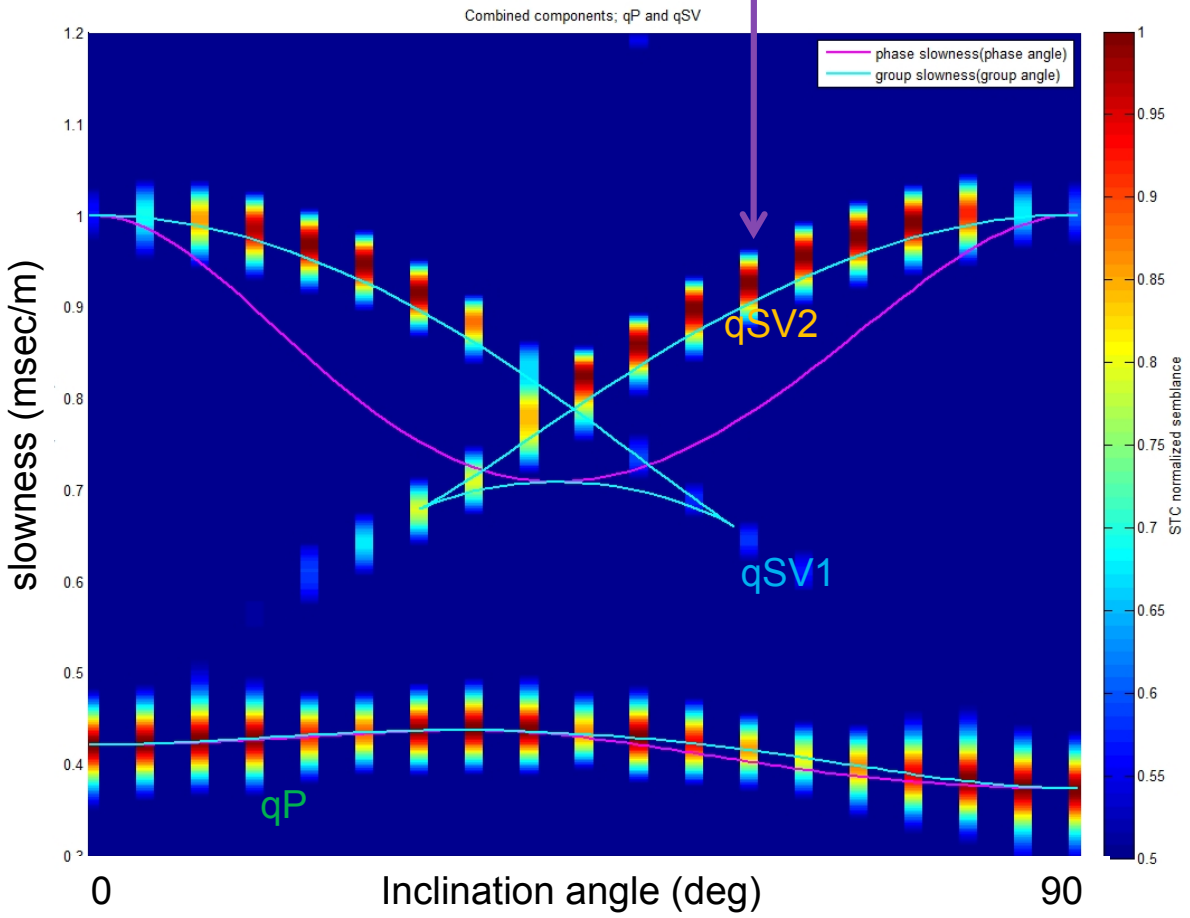

- Here's a combination of inplane and out-of-plane synthetics

- There are three shear arrivals at 60 degrees

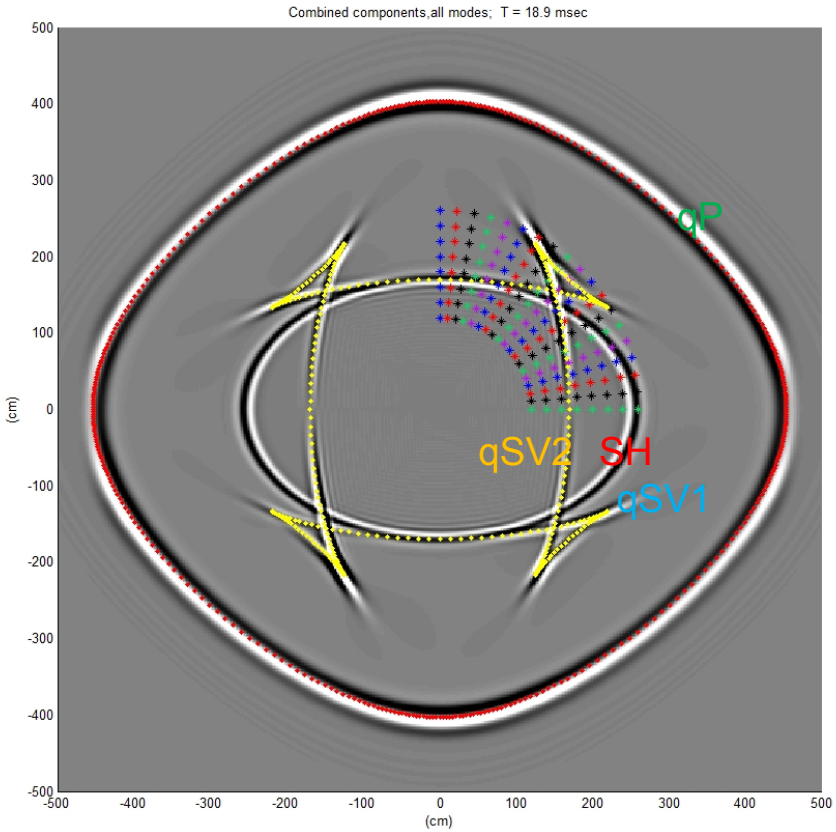

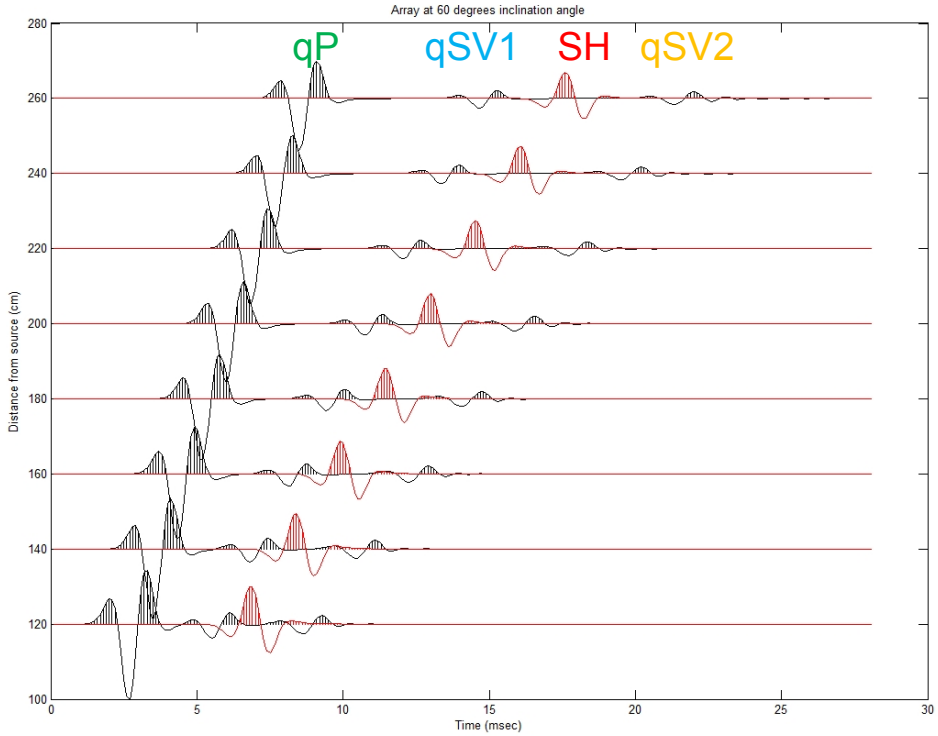

- Three Shears at 60 degrees in combined data
- Slowness values are analytic answer: Group slowness at phase angle whose group angle is 60 degrees

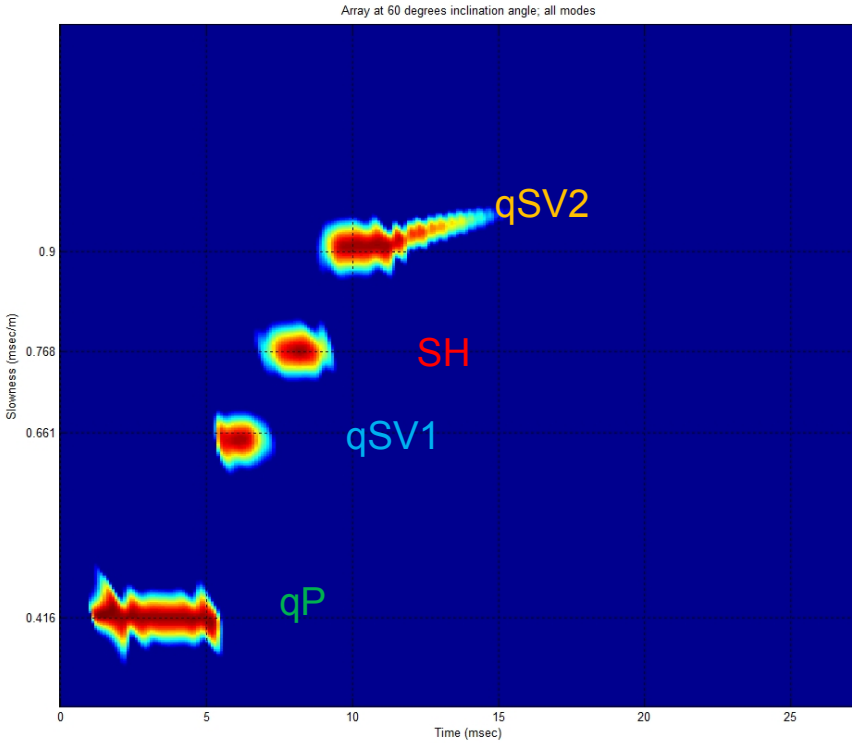

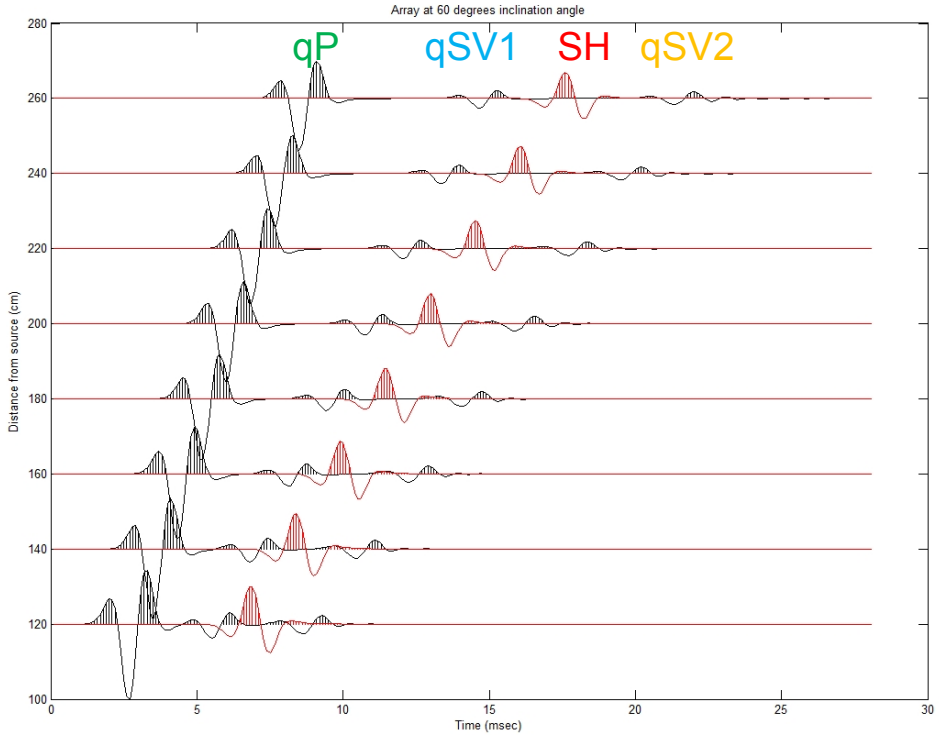

- Introduction of a fluid layer adds complexity, but does not change the STC story (it adds a dispersive Rayleigh arrival)

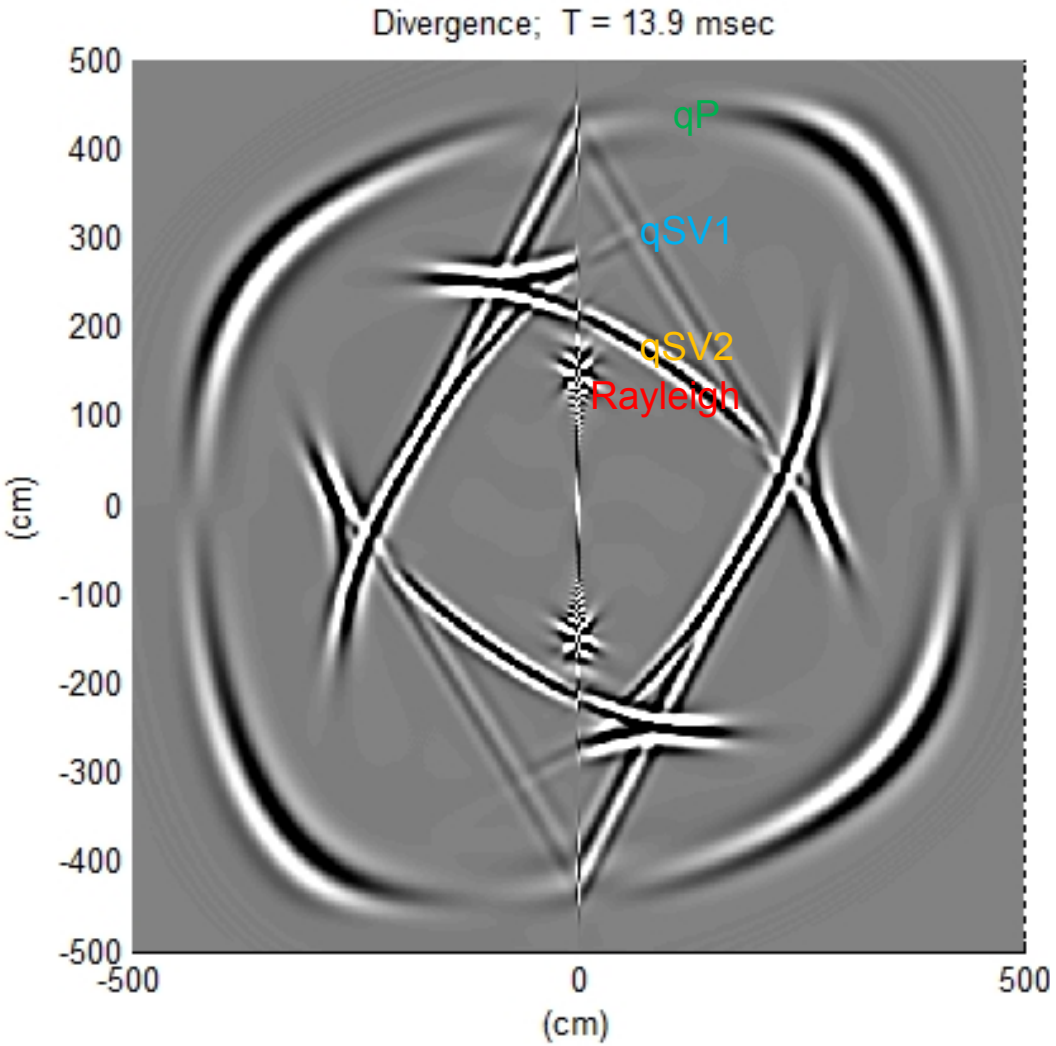

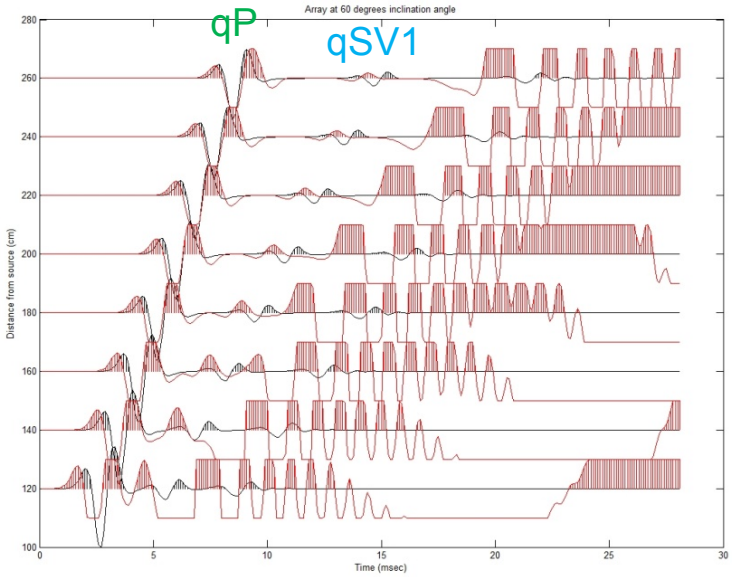

3DFD

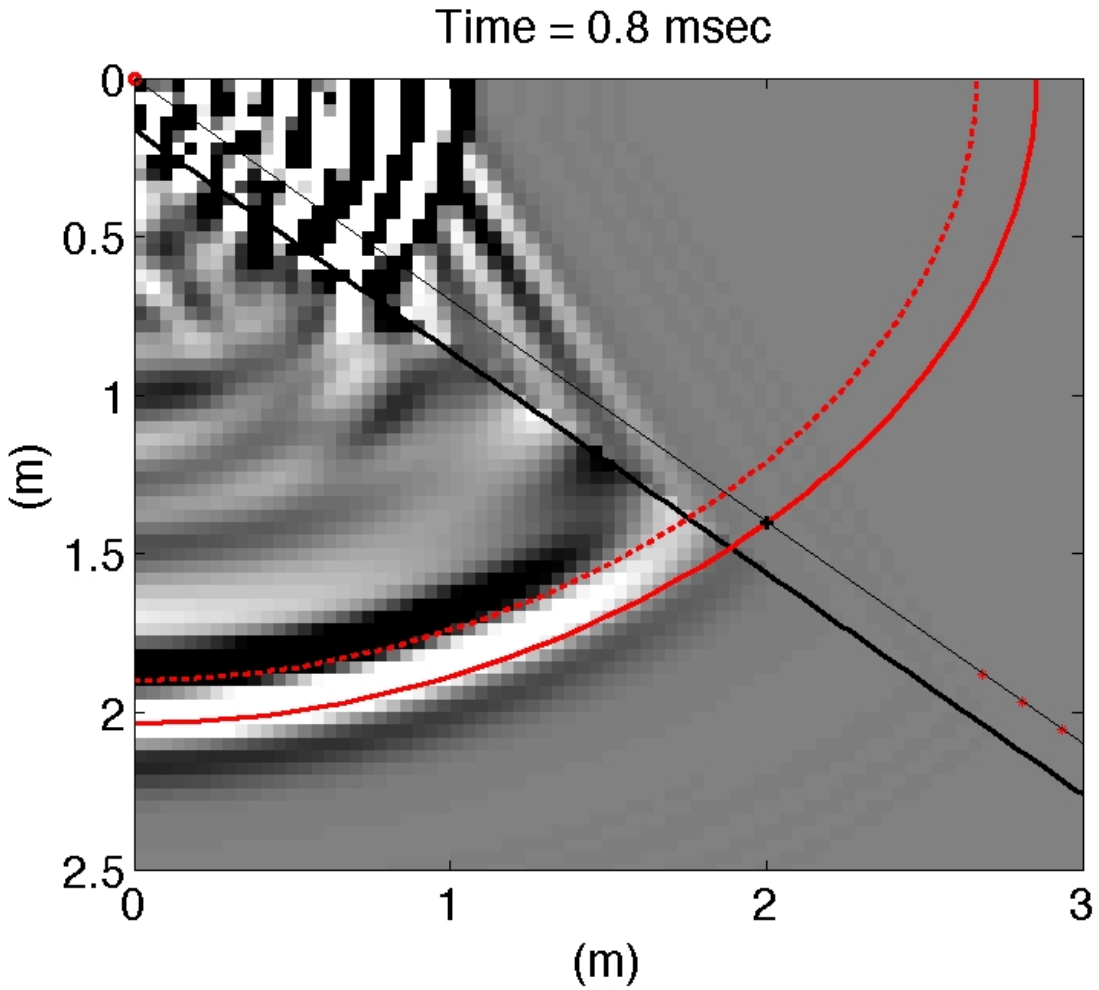

- Monopole source in fluid above an inclined half-space
- Propagation in the solid matches the anisotropic wavefront surface, shedding a headwave.

3DFD

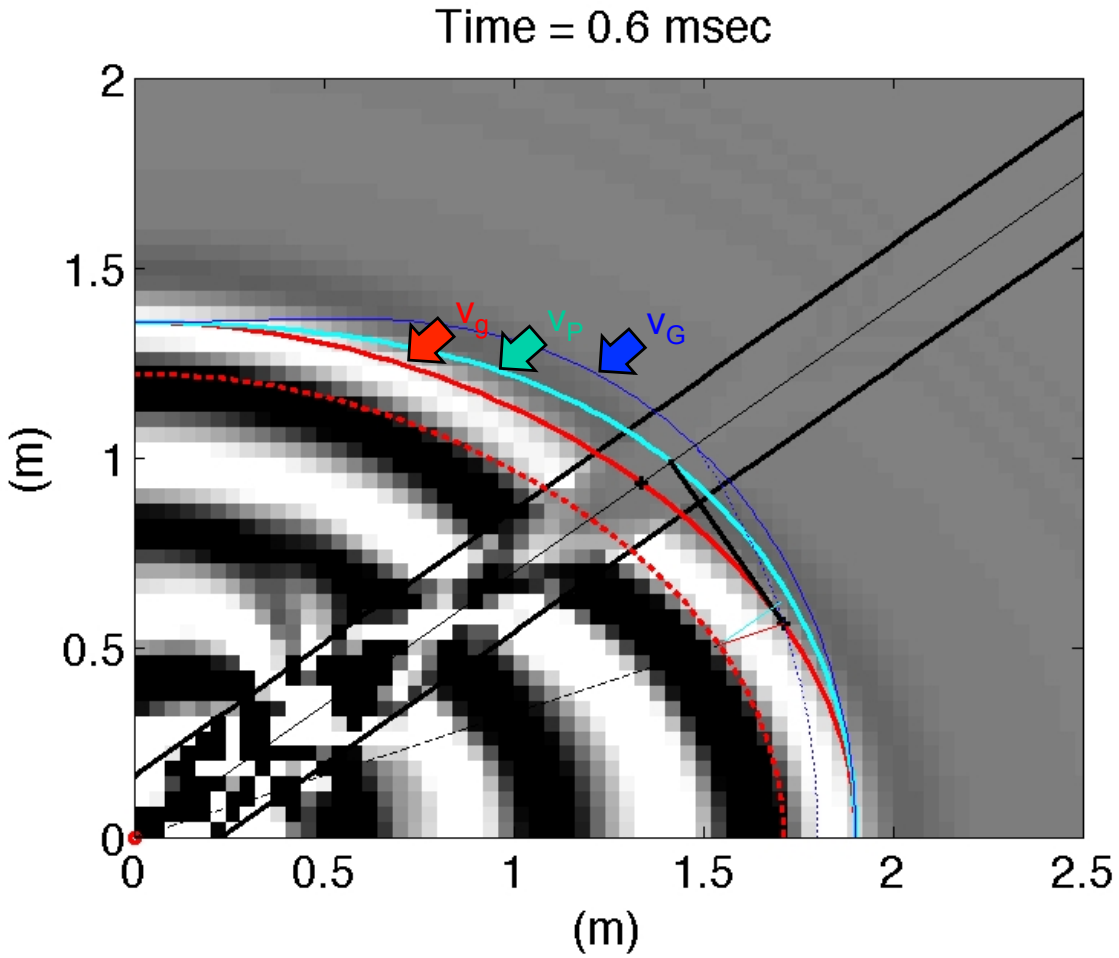

- Monopole source in fluid-filled borehole
- Wavefront in solid couples to reverberant “leaky P’ signal in borehole.
- Signal in borehole slightly lags the wavefront in the solid.

3DFD Processing

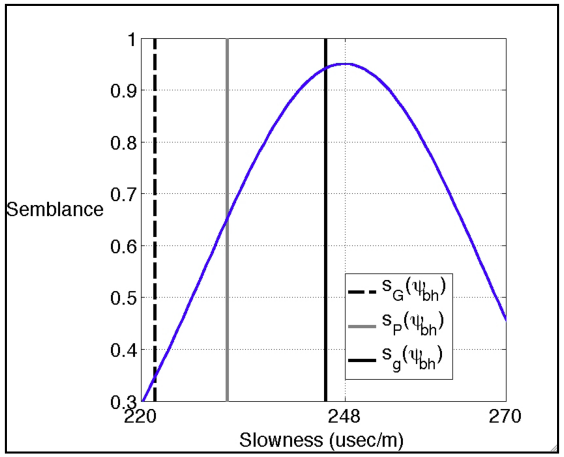

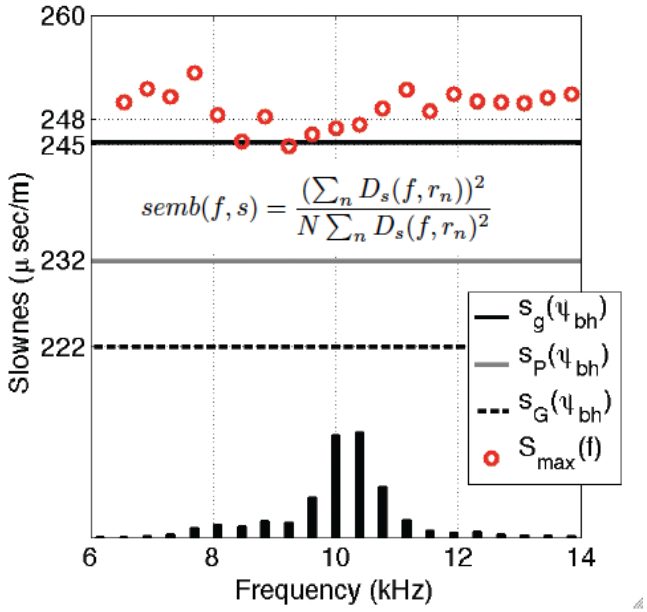

- Waveforms and processing confirm what is evident in the snapshots

- Semblance peaks are about 1% slower than $1/v_g$; 7% slower than $1/v_P$; 12% slower than $1/v_G$.

- Temporal dispersion analysis using a frequency-dependent semblance yields a similar result. Temporal phase slowness at all frequencies is slower than $1/v_g(\psi_{bh})$

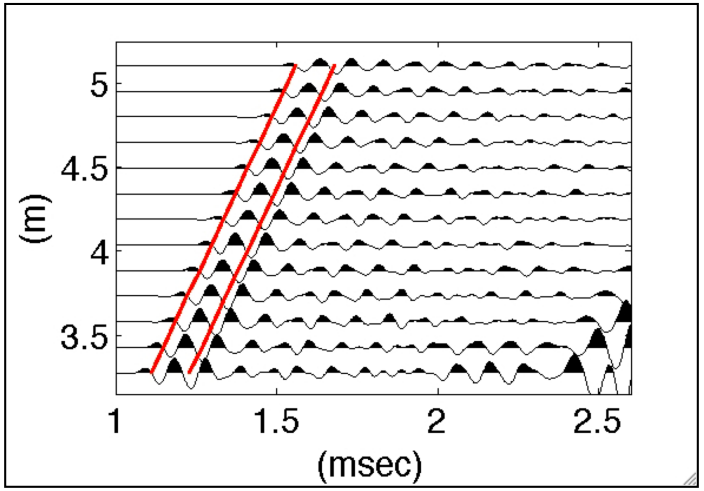

3DFD Processing

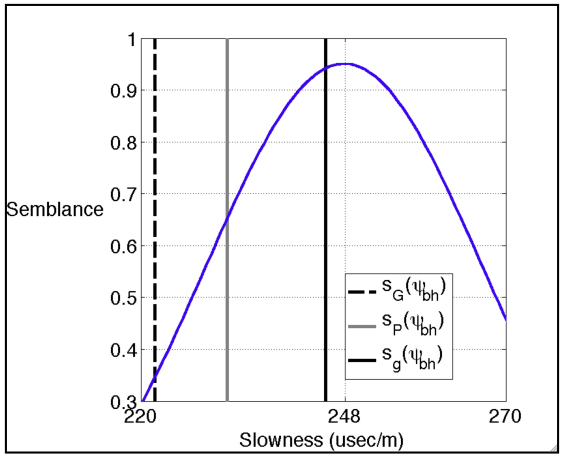

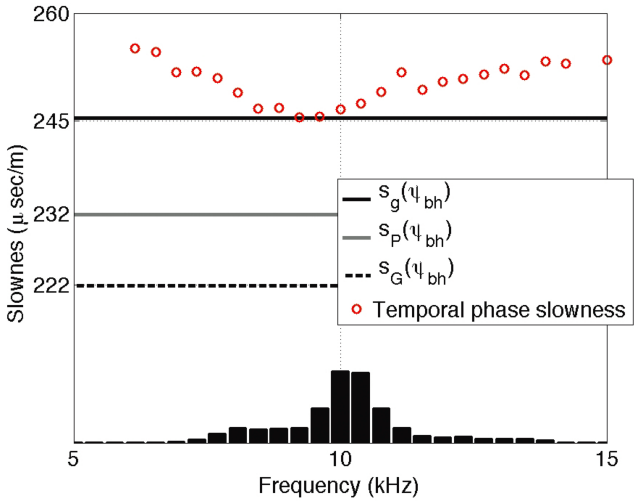

- Waveforms and processing confirm what is evident in the snapshots

- Semblance peaks are about 1% slower than $1/v_g$; 7% slower than $1/v_P$; 12% slower than $1/v_G$.

- Temporal dispersion analysis using the Prony method yields a similar result. Temporal phase slowness at all frequencies is slower than $1/v_g(\psi_{bh})$

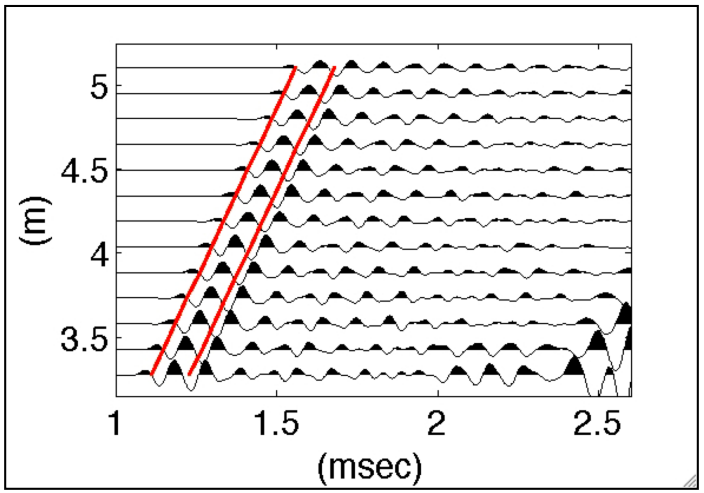

Bias Correction

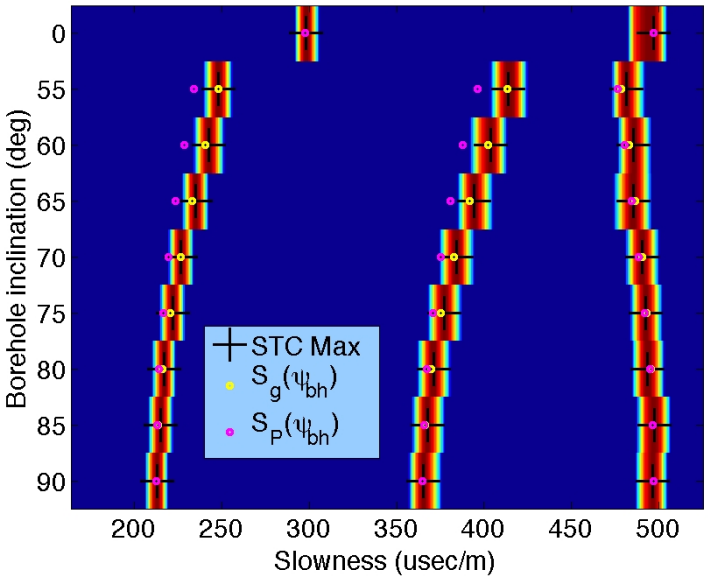

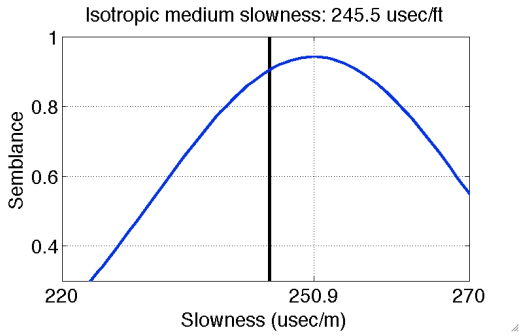

- The small bias between logged slowness and formation slowness is a feature of sonic logs that has always been present.

- Processing all modes and angles in our synthetics, we found that a uniform 2% increase in elastic moduli gave an excellent match between semblance peaks and group slowness.

Modulus	C_{11}	C_{13}	C_{33}	C_{55}	C_{66}
	58.1 $\pm$2.5	16.6 $\pm$1.5	29.6 $\pm$2.0	10.6 $\pm$0.3	19.7 $\pm$0.7

Thomsen	α_0	β_0	ϵ	δ	γ
	3.43 $\pm$0.11	2.05 $\pm$0.05	0.48 $\pm$0.05	0.35 $\pm$.025	0.43 $\pm$.015

Today's Discussion

- Some background on anisotropy:
  - Phase & group vectors
- The Borehole Seismic Example
- The Borehole Sonic Example
  - synthetic data & associated processing
  - field data
- A Fresh Can of Worms

for more details: http://www.mit.edu/~demiller

Log Data from a Gas Shale

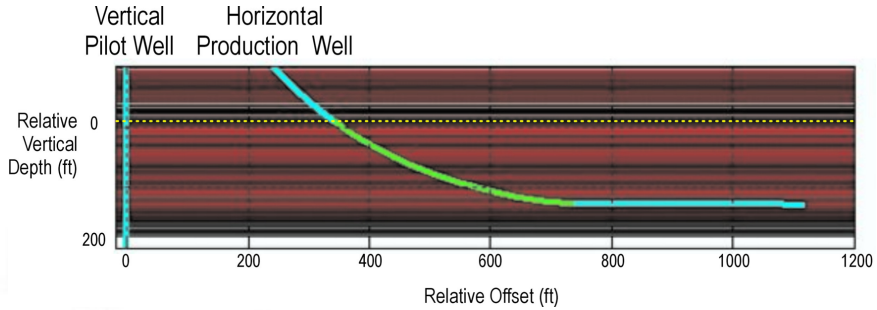

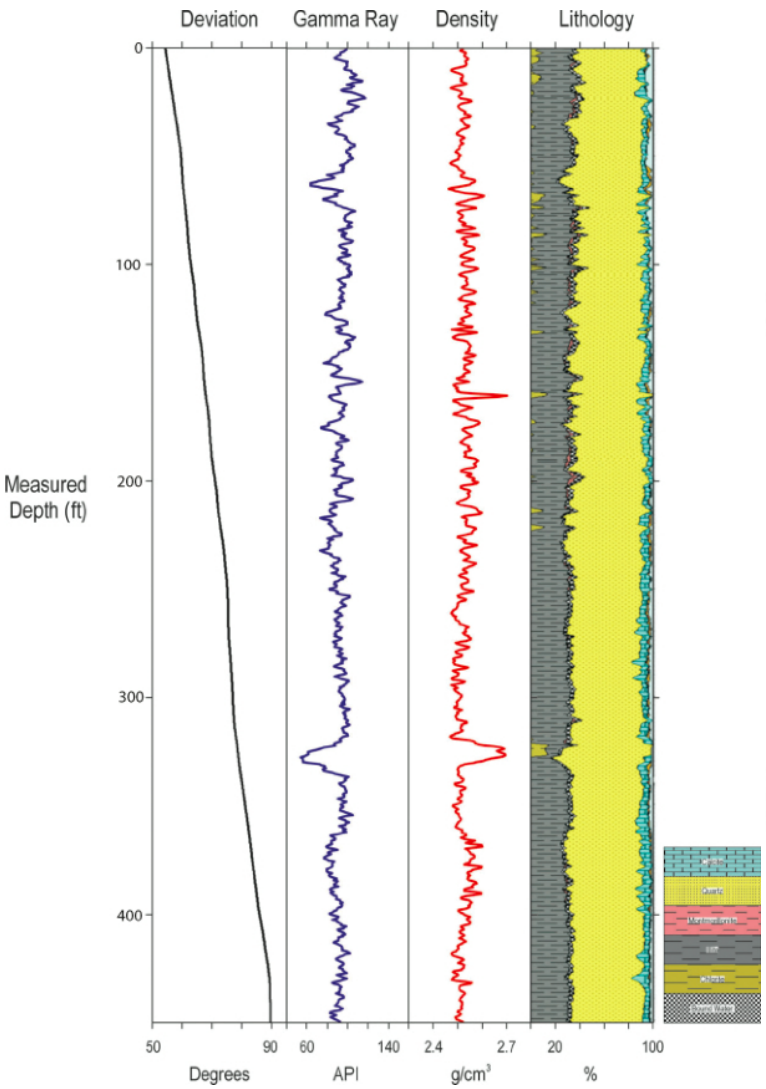

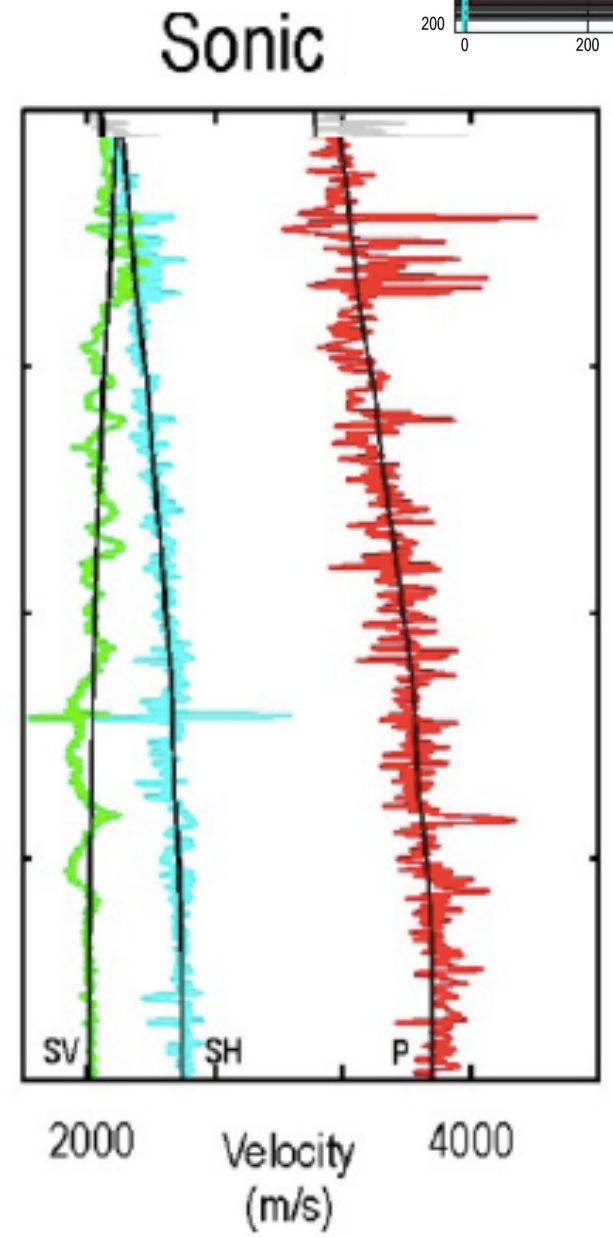

- Standard dipole sonic acquisition & STC processing
- Sonic data are from build section of deviated well
- 63% quartz; 35% clay; 2% calcite

Miller, Horne, Walsh, 1IWRP August 2011

Sonic Log Data from a Gas Shale

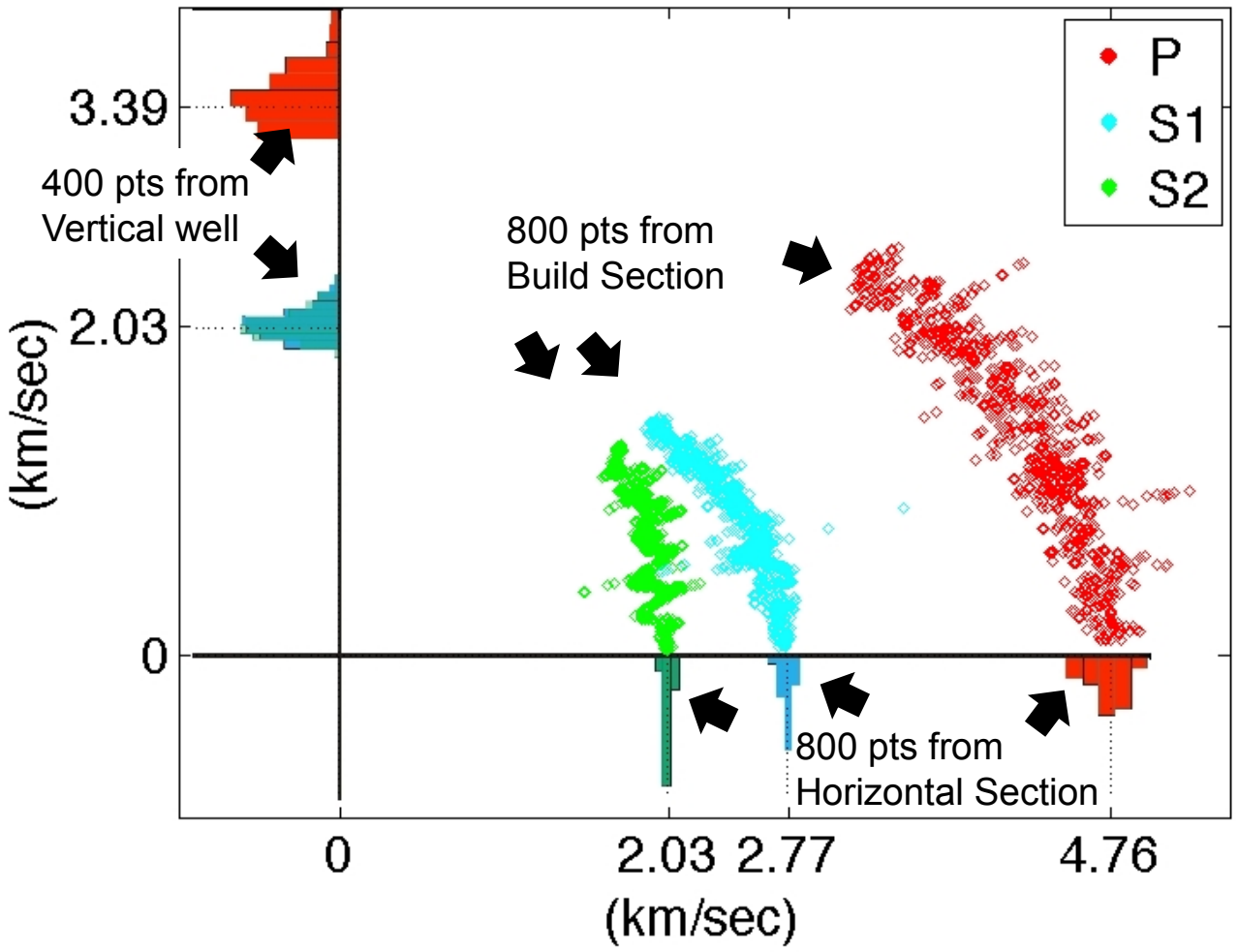

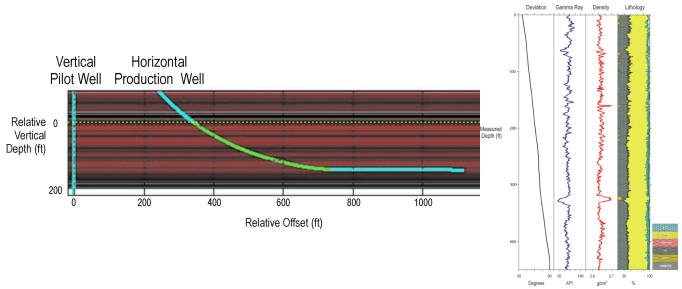

- Standard dipole sonic acquisition & STC processing
- Data from axial sections are summarized by histograms
- Data from build section are plotted at borehole inclination angle
- TI anisotropy, lateral and vertical homogeneity are evident from axial data

Fit by a Single TI Model

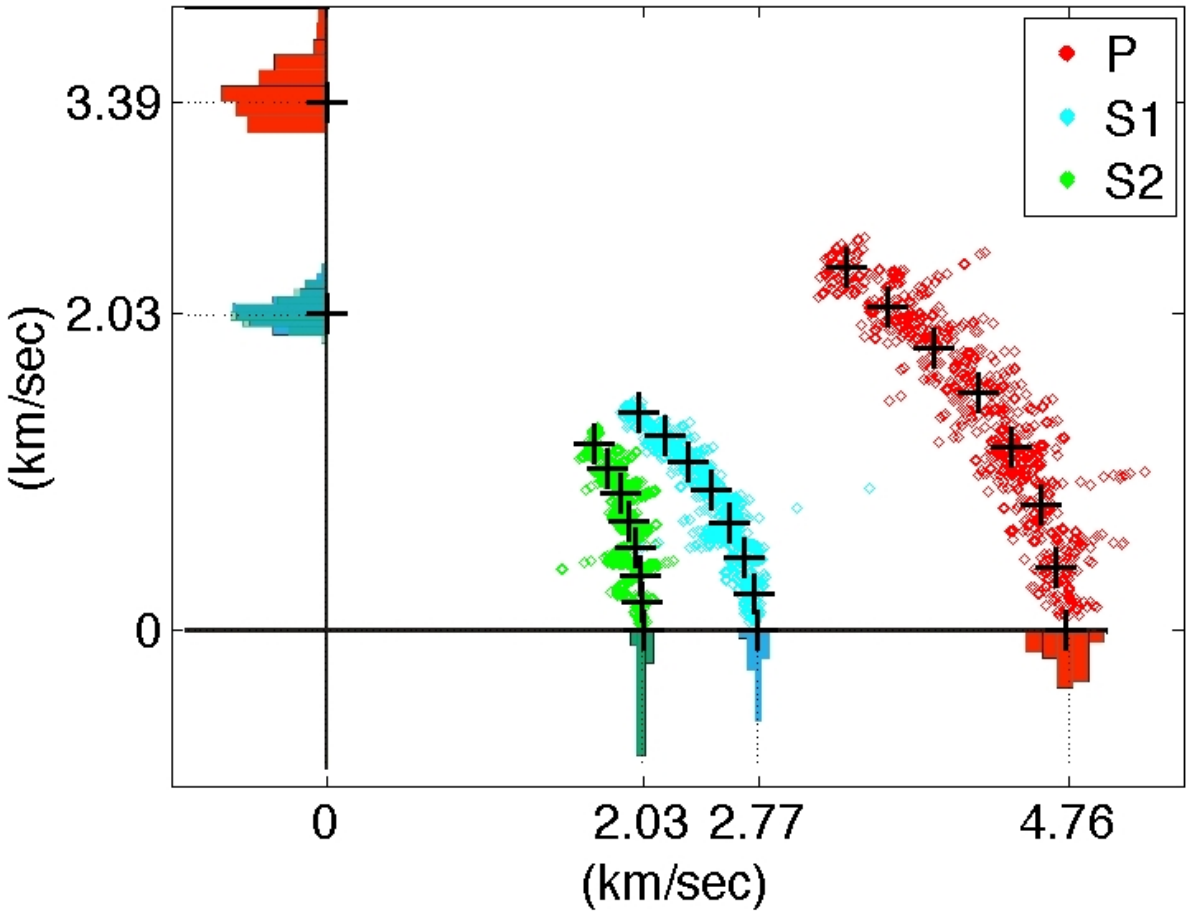

- 3DFD synthetics were created for 9 borehole orientations and 3 modes, then processed with STC

+ Processed 3DFD are plotted at borehole inclination angle

- That's 9000 data points fit with 5 parameters

- We'll describe how the model was obtained, and why it is of particular interest (beyond being a remarkable example of a match between data, *in situ,* and model).

Four Moduli Directly from Axial Data

- C13 remains to be found by a 1-parameter search
- We need to know how C13 relates to off-axis log speeds (i.e. a Correspondence Rule)

	Vertical Well		Horizontal Well			Units
Velocity	V_{33}	V_{31}	V_{11}	V_{13}	V_{12}	
Mean	3.39	2.03	4.76	2.03	2.77	km/sec
RMS variation	0.13	0.07	0.11	0.03	0.05	km/sec

Modulus	C_{33}	C_{55}	C_{11}	C_{66}	
	29.0	10.4	57.0	19.3	GPa

Thomsen	α_0	β_0	ϵ	γ
	3.39	2.03	0.48	0.43

density	ρ	kg/m^3
	2520	

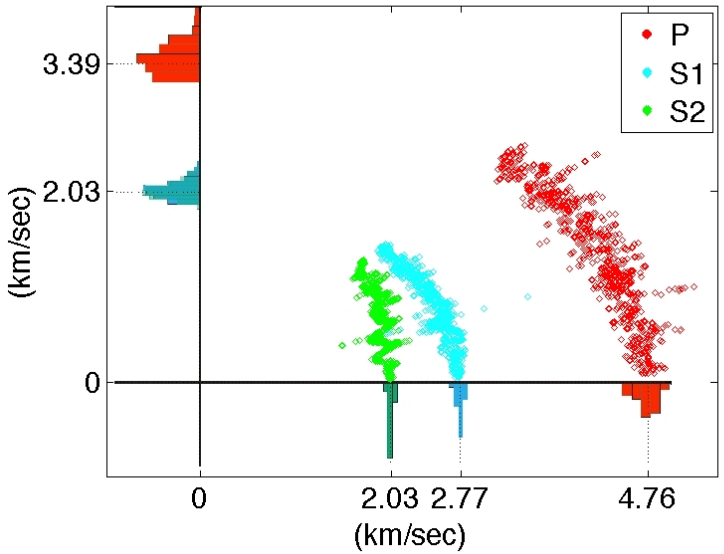

An Important Point

• There has been confusion in the literature regarding interpretation of sonic logs in deviated wells in anisotropic media. Because wavefronts radiated from a point source are not generally spherical, there has been uncertainty about whether borehole inclination should be matched to ray direction (group angle) or wavefront normal direction (phase angle).

Our data clearly show that, at least for fast anisotropic formations such as this gas shale, sonic logs measure **group slowness** for propagation with the **group angle equal to the borehole inclination angle**. The data are inconsistent with an interpretation that they measure phase slownesses for propagation with phase angle equal to borehole inclination angle.

The confusion in the literature stemmed from a failure to properly distinguish group slowness as a function of **group angle** from group slowness as a function of **phase angle**.

Correspondence Rules: Hornby & Sinha

SEG Expanded Abstracts 2003
Do We Measure Phase Or Group Velocity With Dipole Sonic Tools?
B. Hornby, X. WANG And K. Dodds

Comparisons of the computed velocities with the theoretical wave surfaces clearly shows the best fit with the group velocity surfaces. And so ***we conclude that we are measuring the group velocity*** *for all wave modes excited by the dipole sonic tool.*

GEOPHYSICS, 71(6) 2006 191–202
Elastic-wave propagation in deviated wells in anisotropic formations
B. Sinha, E. Şimşek, and Q. Liu

Processing of synthetic waveform*s in deviated wellbores using a conventional STC algorithm or a modified matrix pencil algorithm* ***yields phase slownesses*** *of the compressional and shear waves propagating in the nonprincipal directions of anisotropic formations.*

The full-wave processing of dipole sonic logs using slowness time coherence has been demonstrated to yield phase rather than group velocities of compressional Vp and shear Vs waves (Sinha et al., 2006). This finding is imperative to the problem discussed in this paper because the angle dependence of phase and group velocities in anisotropic media can be quite different (Thomsen, 1986; Vernik and Liu, 1997).

- Vernik 2008, Geophysics

Proposed Correspondence Rules:

(GG) *Logs measure **group slowness** for propagation with the **group angle** equal to the borehole inclination angle* (Hornby et al. 2003)

(PP) *Logs measure **phase slowness** for propagation with the **phase angle** equal to the borehole inclination angle* (Sinha et al. 2006)

When anisotropy is strongly present, these rules are incompatible. For the case at hand, (GG) is uniquely consistent with the data and matching synthetics. Sinha et al. reached their conclusion by confusing Hornby's rule with a different one:

(GP) *Logs measure **group slowness** for propagation with the **phase angle** equal to the borehole inclination angle* (Sinha et al. 2006)

That is, Sinha et al. compared v_P with v_G rather than with v_g.

SH Comparison

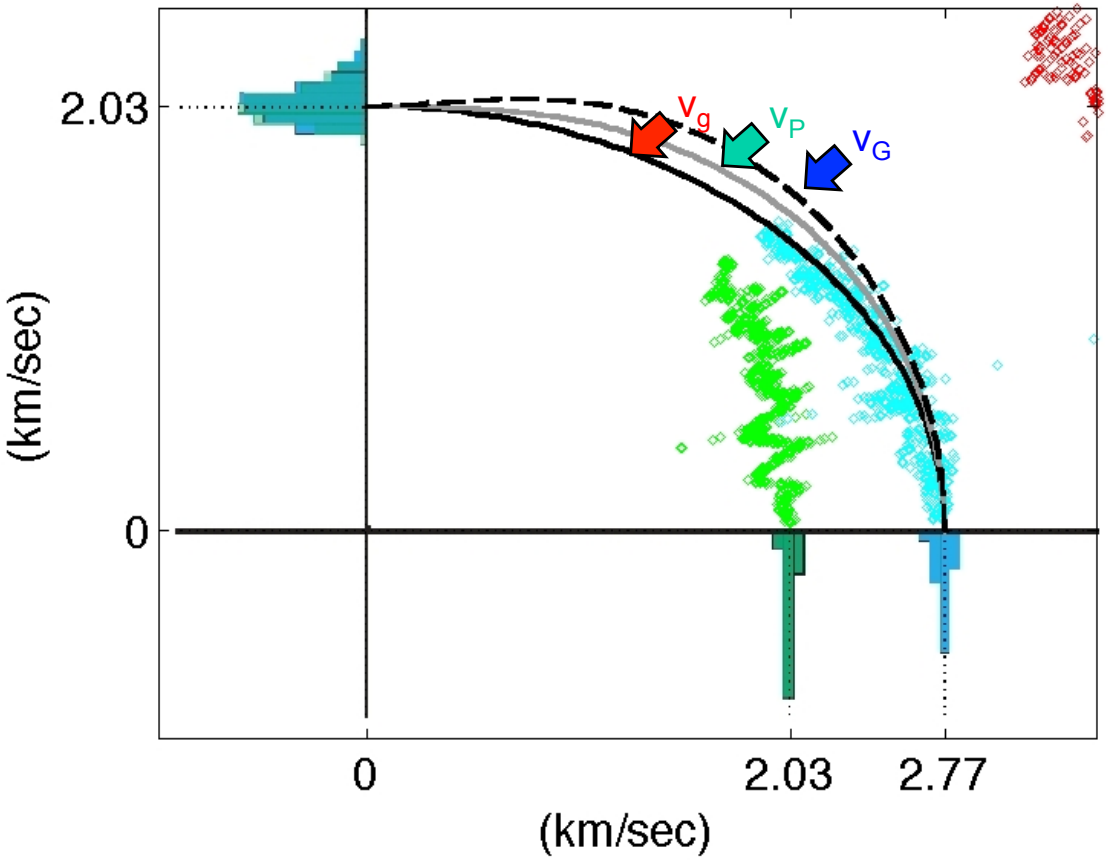

- There are no adjustable parameters. Curves are determined by shear slowness from horizontal well.
- (GG) fits. (PP) and (GP) do not.
- (GG) RMS misfit is .029 km/sec
- (PP) RMS misfit is .082 km/sec

SH phase vectors form an ellipse in slowness not in velocity
SH group vectors form an ellipse in velocity not in slowness
These data form an ellipse in velocity not in slowness

C13

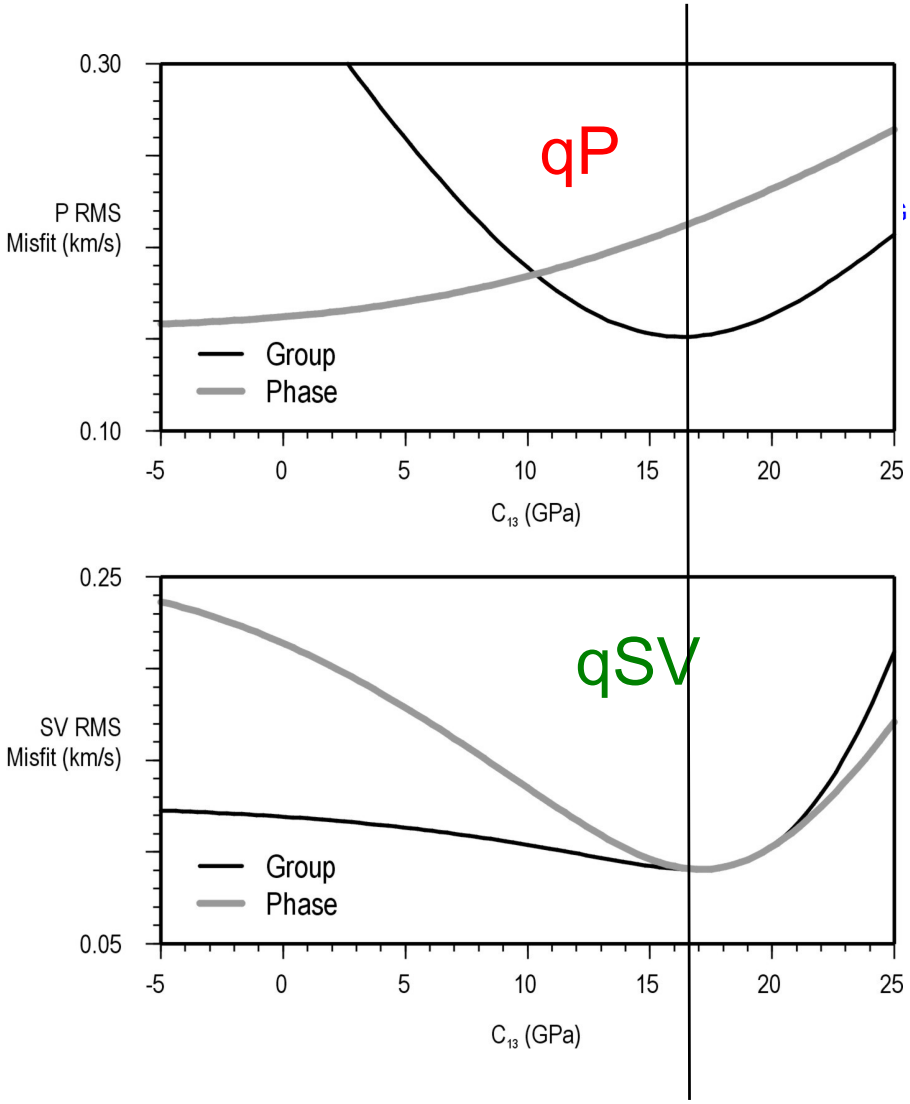

- Figures at left show RMS misfit as a function of C13 for (GG) in black, (PP) in gray.
- (GG) fits both modes at C13 = 16.4 GPa
- (PP) does not give a consistent answer
- qSV best fit agrees with (GG) because, in this case, qSV phase and group surfaces are nearly coincident.
- (PP) best fit for qP is physically unreasonable, -5 GPa.

(GG) Best Fit

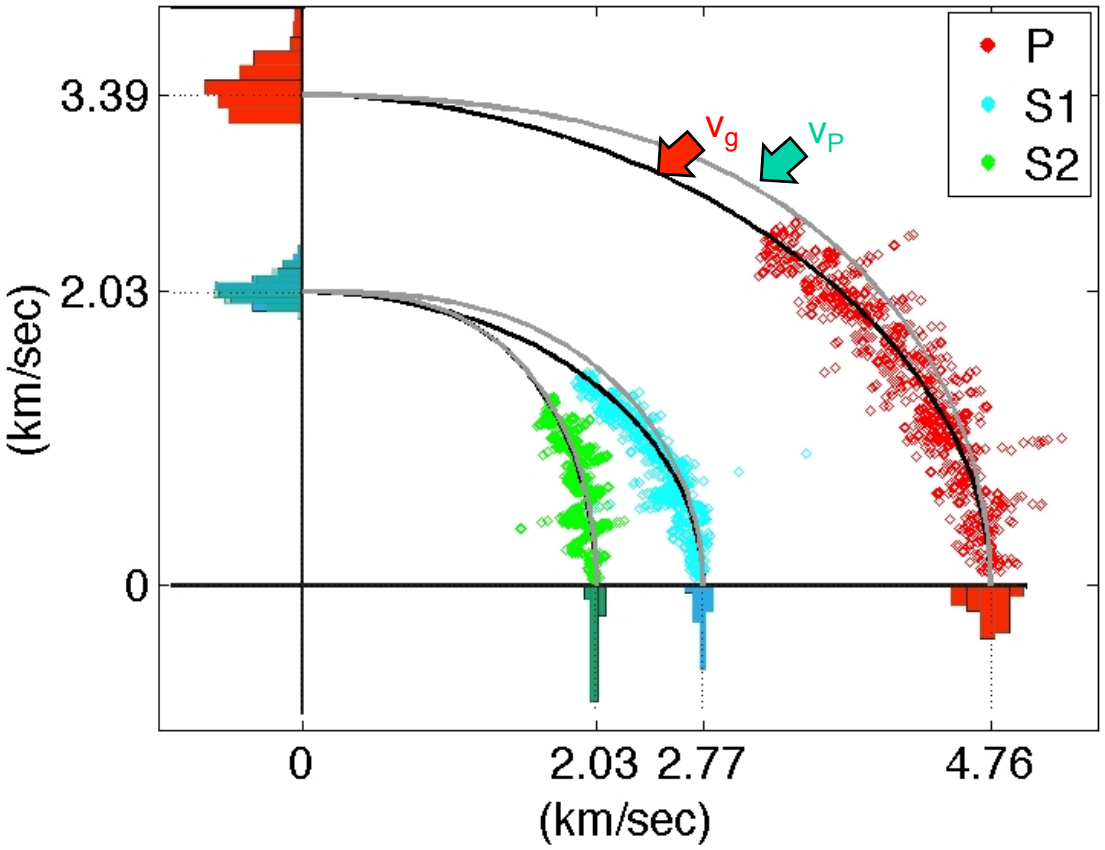

- v_g in black, v_P in gray, for each mode, using the (GG) best-fit value, C13 = 16.4 GPa

- (GG) fits all modes

- (PP) only fits qSV, (where phase and group surfaces happen to coincide).

(PP) Fit to qP Data

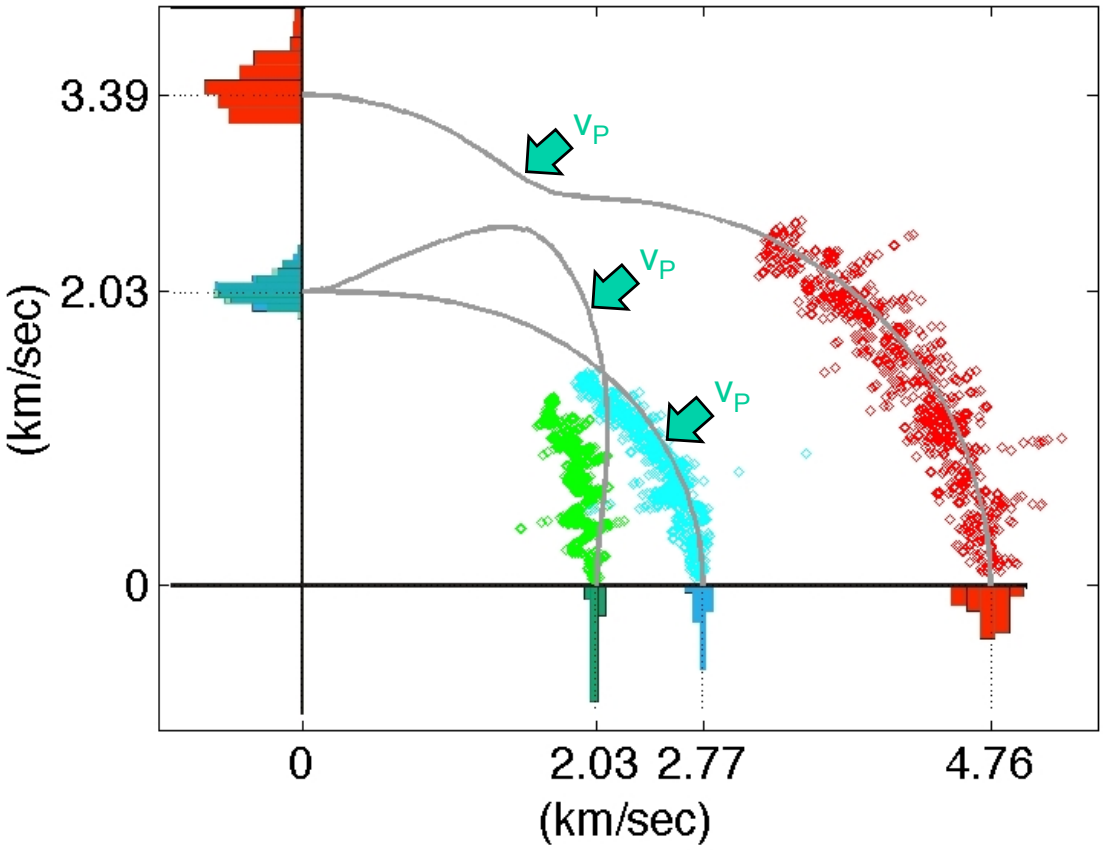

- v_P in gray for each mode, using the value C13 = -5 Gpa, which fits the qP data with the phase surface.

- qSV is egregiously misfit, with coincident shear speeds predicted at 55 degrees.

Best-Fit and 4-Parameter Approximations

Annie1: C13/C12 = 0.45 C13/C33 = 0.28

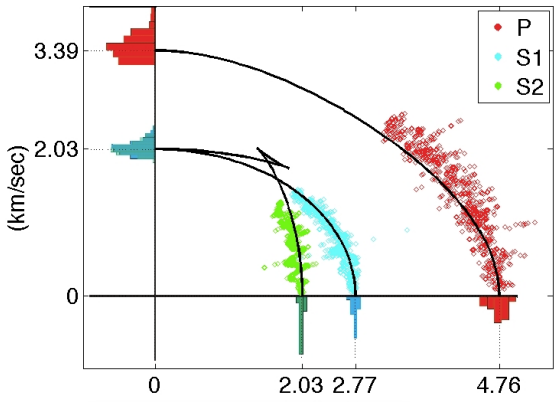

δ = 0;
C13 = C33 – 2 C55

Fractured Isotropic: C13/C12 = 0.59 C13/C33 = 0.37

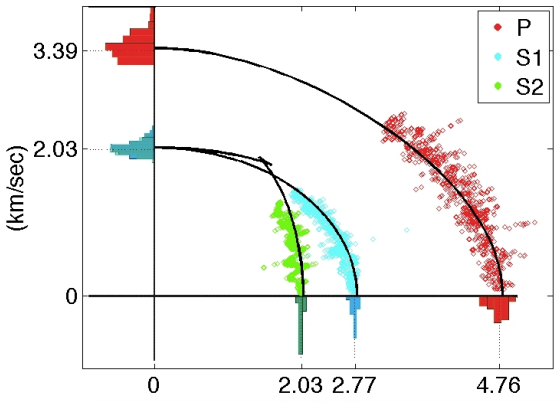

δ = .1;
C13 = -C66 + sqrt($C66^2$ + C12 C33)

Best Fit: C13/C12 = 0.89 C13/C33 = 0.57

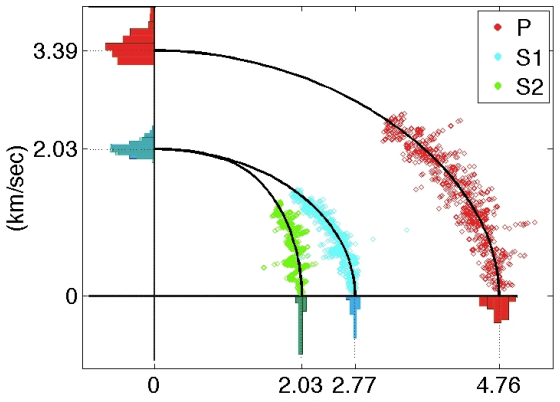

δ = .35;
C13 = 16.4 GPa

Annie2: C13/C12 = 1 C13/C33 = 0.63

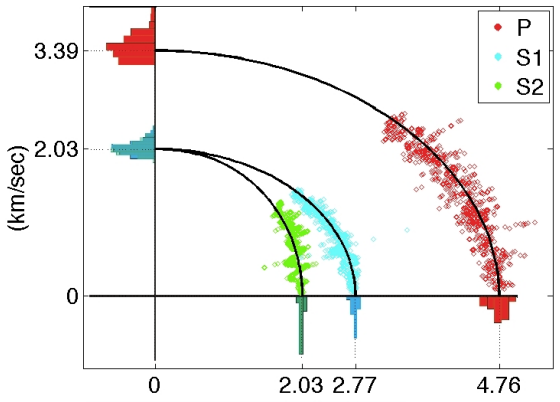

δ = .45;
C13 = C11 – 2 C66

Elliptical: C13/C12 = 1.03 C13/C33 = 0.66

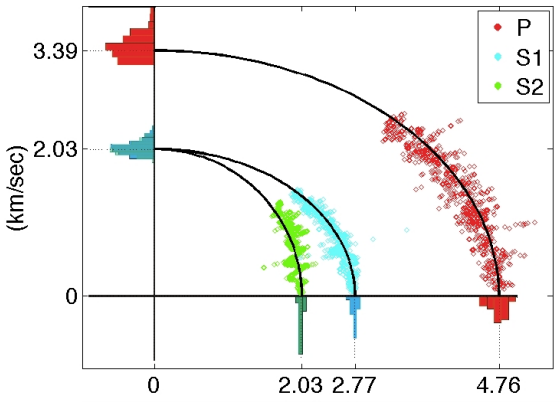

δ = ε=.48;
C13 = sqrt(C11 – C55) (C33 – C55))

QuasiElliptical: C13/C12 = 1.21 C13/C33 = 0.77

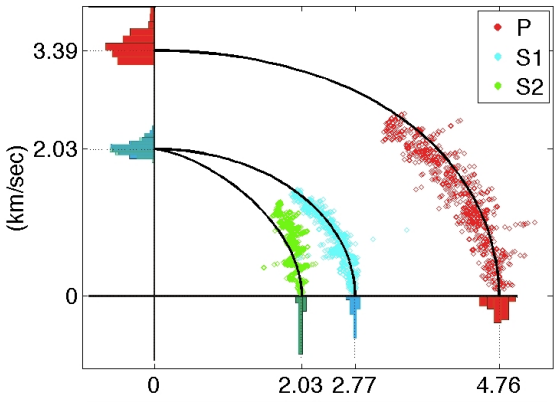

δ = .54;
C13 = (C11 + C33)/2 – 2 C55

Best-fit Parameters

Modulus	C_{11}	C_{13}	C_{33}	C_{55}	C_{66}
	57.0 $\pm$2.5	16.4 $\pm$1.5	29.0 $\pm$2.0	10.4 $\pm$0.3	19.3 $\pm$0.7

Thomsen	α_0	β_0	ϵ	δ	γ
	3.39 $\pm$0.11	2.03 $\pm$0.05	0.48 $\pm$0.05	0.35 $\pm$.025	0.43 $\pm$.015

Concluding Remarks

1) Log data from this field example are remarkably consistent with the rule that sonic logs measure **group slowness** for propagation with the **group angle equal to the borehole inclination angle**. The data are inconsistent with an interpretation that they measure phase slownesses for propagation with phase angle equal to borehole inclination angle.

2) Processed 3DFD synthetics simulating best-fit model confirm the interpretation.

3) The best-fit model is close to satisfying the second Annie condition C13 = C12, as well as the elliptical condition, $\varepsilon = \delta$.

4) Data from deviated well alone would have been sufficient (but less convincing).

5) See the extended abstract for more details. I'll put a copy at www.mit.edu/~demiller

Thanks to:

- Coauthors Steve Horne and John Walsh
- Yang Zhang at MIT, Earth Resources Lab for help installing the 3DFD cone on my Mac mini
- Phil Christie, David Johnson, Chris Chapman for helpful comments
- The operating company for permission to show the data

Some shales

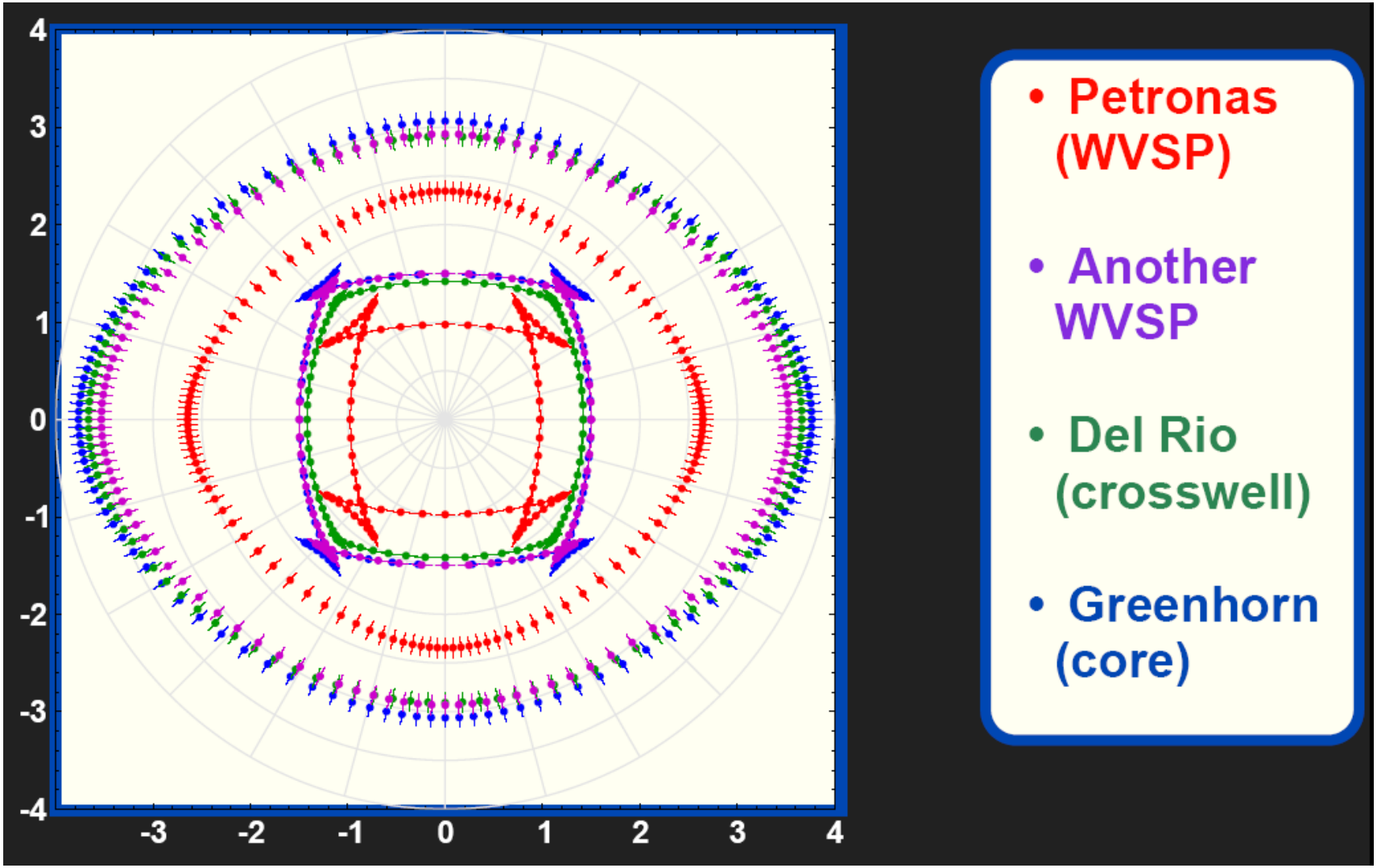
4
3
2
1
0
-1
-2
-3
-4
-3
-2
-1
0
1
2
3
4
• Petronas (WVSP)
• Another WVSP
• Del Rio (crosswell)
• Greenhorn (core)

Today's Discussion

- Some background on anisotropy:
  - Phase & group vectors
- The Borehole Seismic Example
- The Borehole Sonic Example
  - synthetic data & associated processing
  - field data
- A Fresh Can of Worms

for more details: http://www.mit.edu/~demiller

Anisotropic static and dynamic moduli measured on shale plugs cut parallel and perpendicular to bedding

or

Serendipity in the quest for C13

Doug Miller[1], *Richard Plumb*[2] and Greg Boitnott[3]

1st International Workshop on Rock Physics

Denver, CO August 7-12, 2011

[1] MIT-E.A.P.S., [2] Plumb Geomechanics & MIT-C.E.E., [3] New England Research

Serendipity Event#1

Found sample of the problem rock

Shale Sample of Opportunity

Bedding enhanced by erosion by water

Conchoidal-like fracture surface

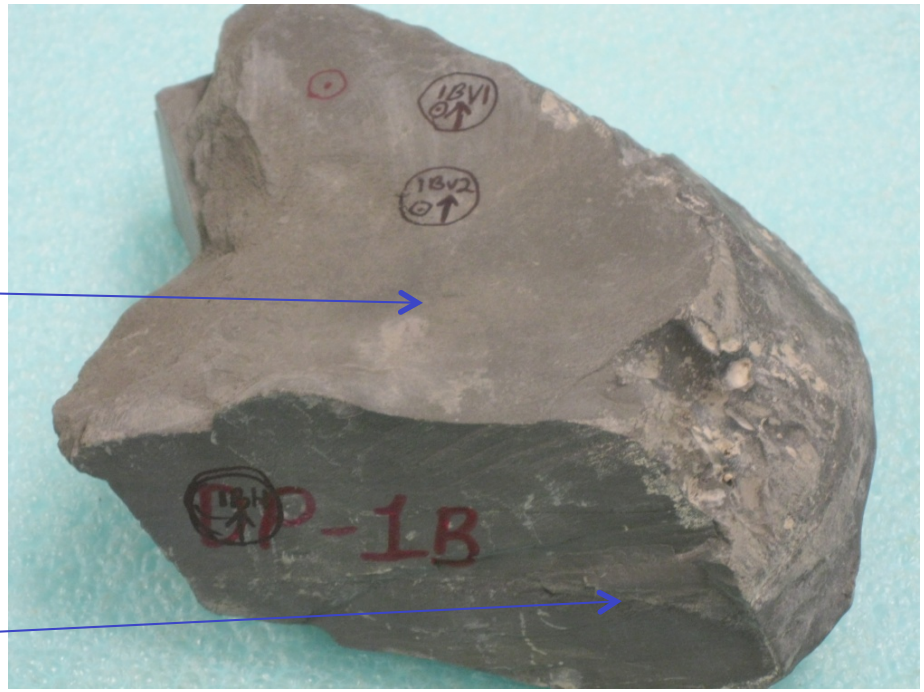

1”

scale

Weak compositional layering

Sample Characterization

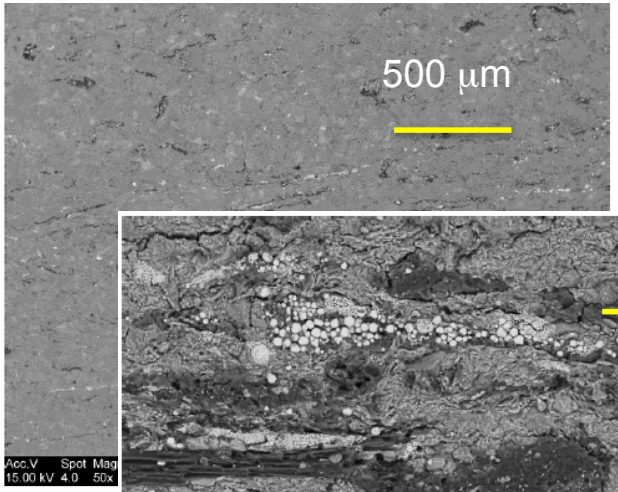

Visually homogeneous

Bulk density:	2.38 gm/cc
Grain denisty:	2.62 gm/cc
Porosity:	9%

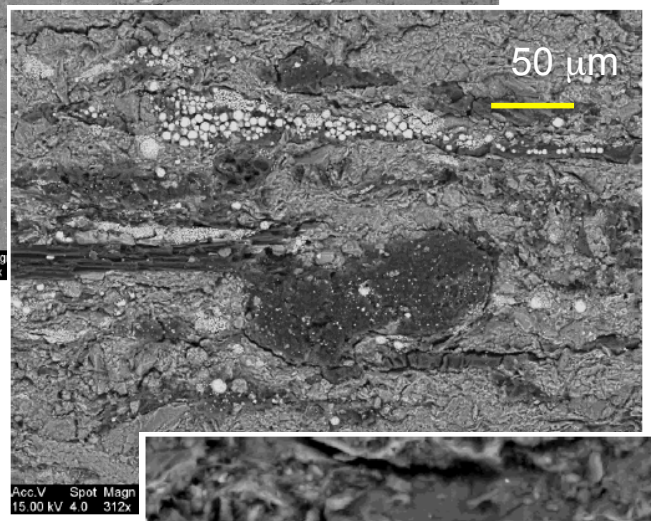

Inclusions of organic matter (dark) and pyrite (white) reveal bedding plane

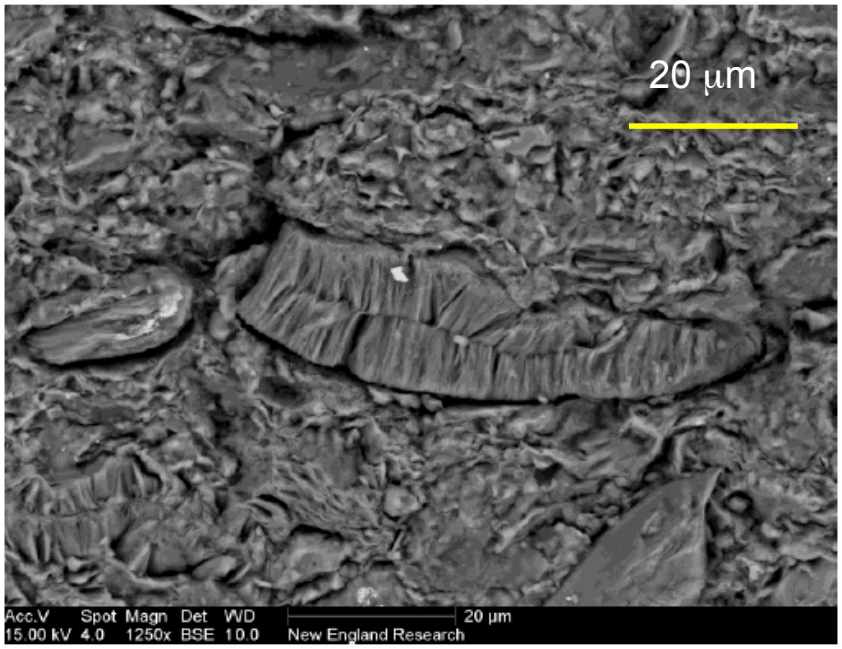

High volume fraction of clay minerals with few detrital grains. Interparticle Porosity is now visible. Evidence of mechanical compaction but no cementation

Instrumentation

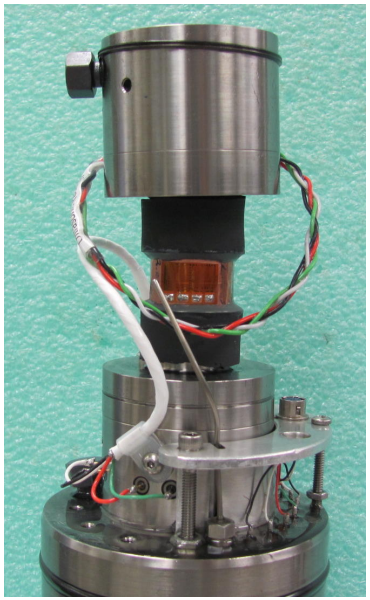

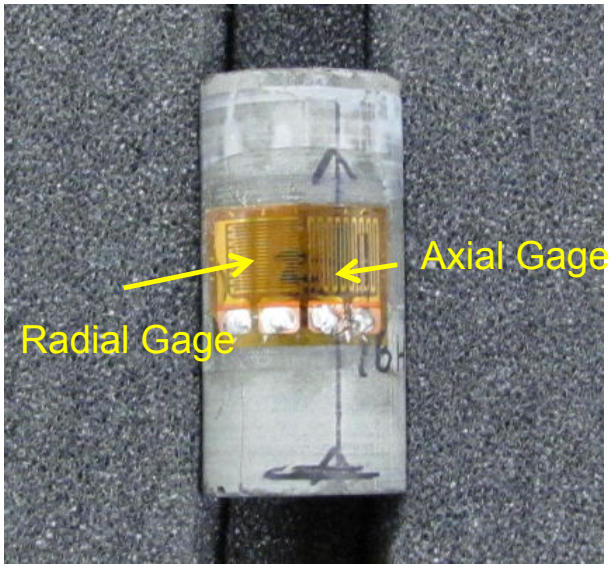

0.75”

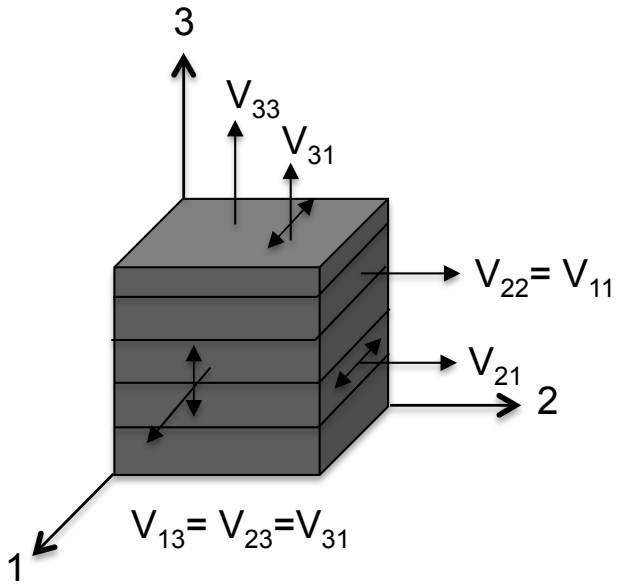

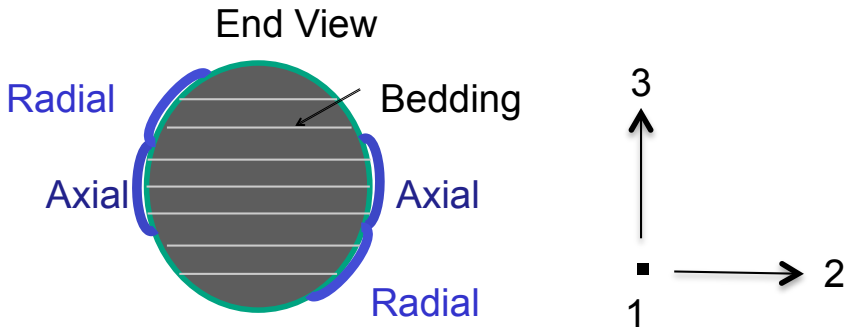

Experimental Protocol

3 plugs perpendicular to fabric

3 plugs parallel to fabric

Confining pressure 0, 20, 40 MPa

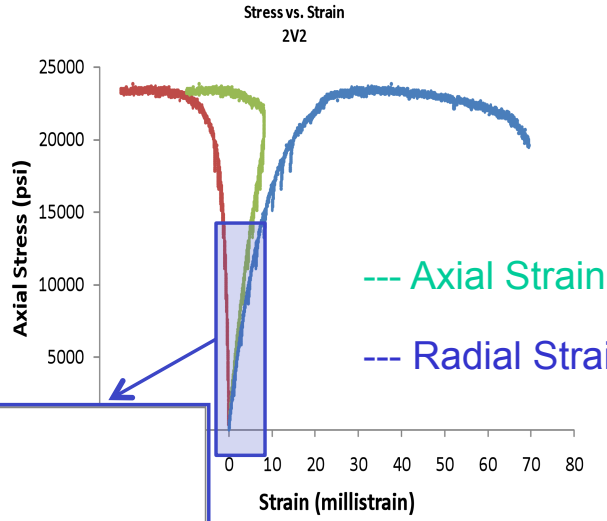

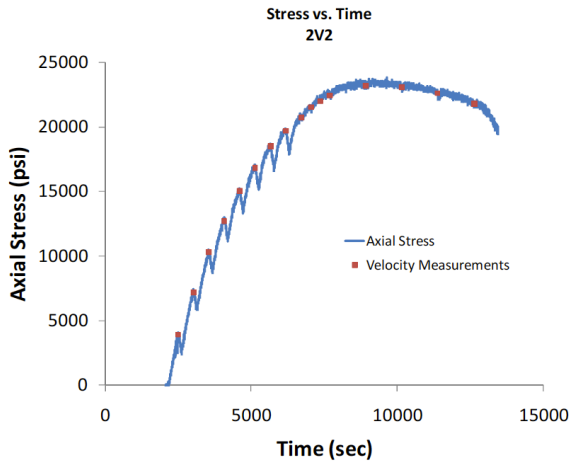

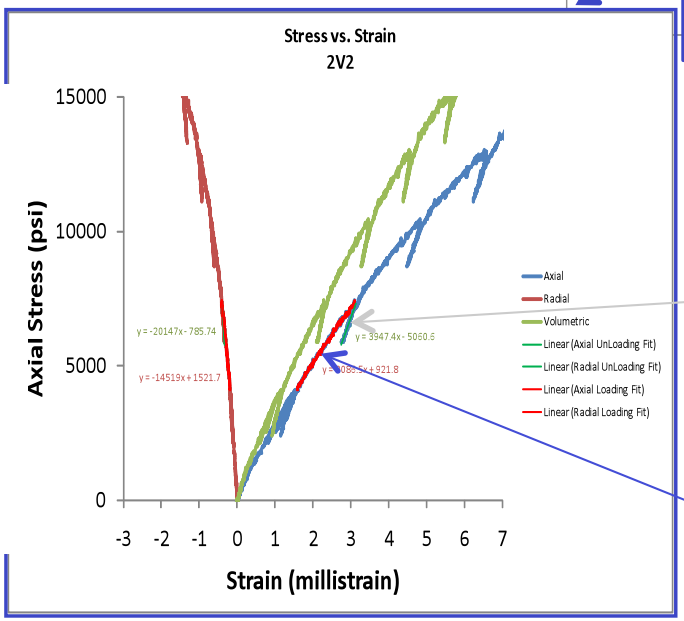

Unloading segment for moduli computations

Loading segment for moduli computations

TI parameters from ultrasonics

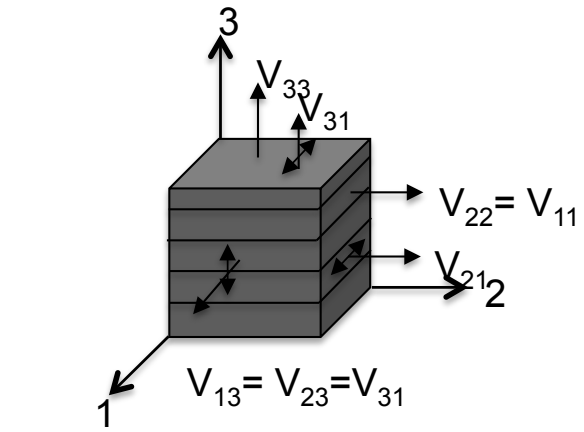

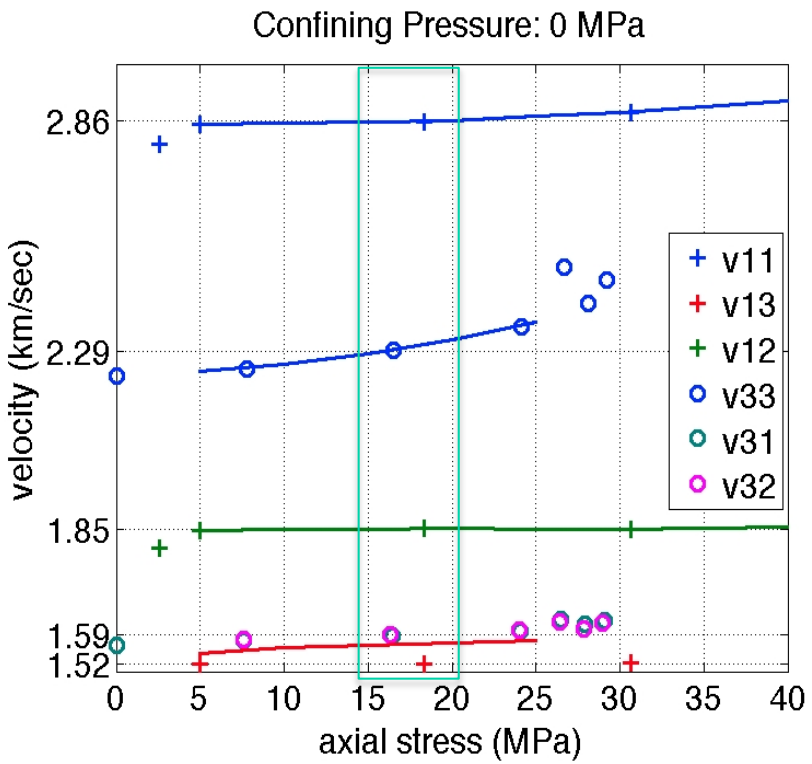

Theory and Measurement

1. $V11^2 = C11/\rho$
2. $V33^2 = C33/\rho$
3. $V12^2 = C66/\rho$
4. $V13^2 = V31^2 = V32^2 = C55/\rho$

For TI symmetry: C12 + 2 C66 = C11.

Thus, ultrasonics determine C33, C55, C11, C12, C66 (but not C13)

ρ = 2374 kg/m^3
V33 = 2.29 km/sec
V11 = 2.86 km/sec
V31 = 1.52 km/sec
V32 = 1.59 km/sec
V13 = 1.85 km/sec

C33 = 12.5 Gpa
C11 = 19.4 Gpa
C55 = 5.7 Gpa
C12 = 3.1 Gpa
C66 = 8.2 GPa

TI parameters from load-unload cycles

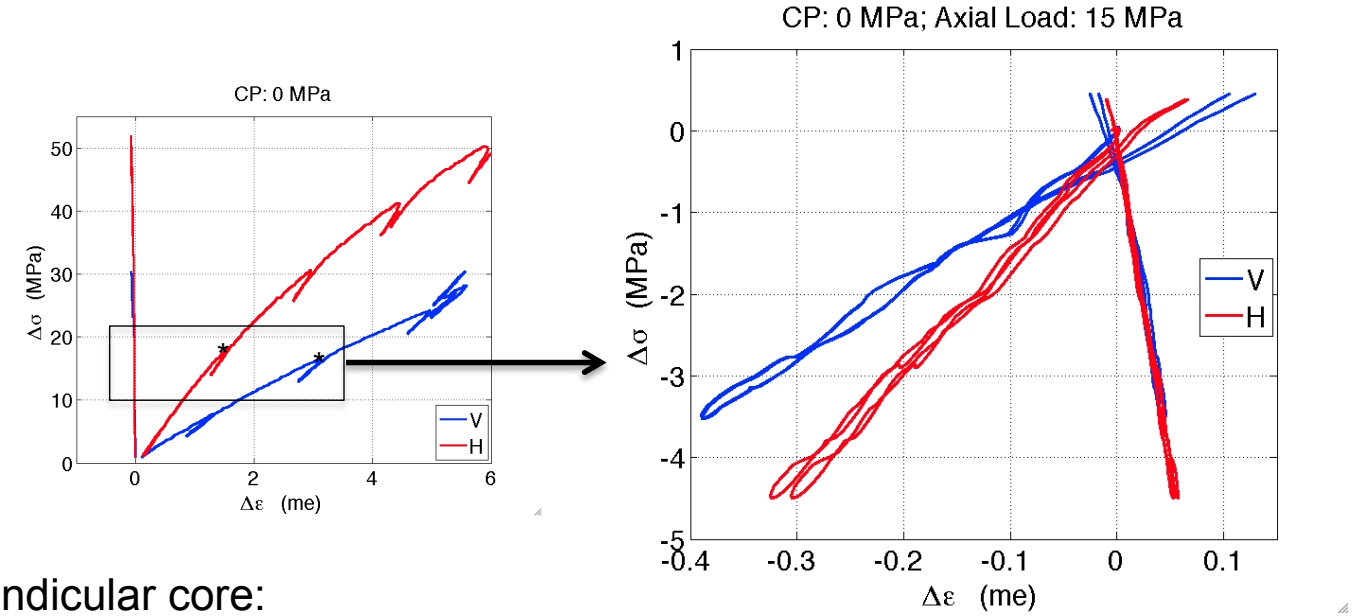

Theory:

Perpendicular core:

- axial stress/axial strain = σ33/ε33 = 1/S33 = E33
- axial stress/radial strain = σ33/ε11 = 1/S13 = E33/ν33

Parallel core

- axial stress/axial strain = σ11/ε11 = 1/S11 = E11
- axial stress/radial strain@45° = 2 σ11/(ε33+ε11) = 2/(S13+S12)

Observe in this case: 1/S12 = 2/(S13+S12), hence S12 = S13.

Statics determine S33, S13, S11, S12, & thence C33, C13, C11, C12, C66 (but not C55)

Combined Methods

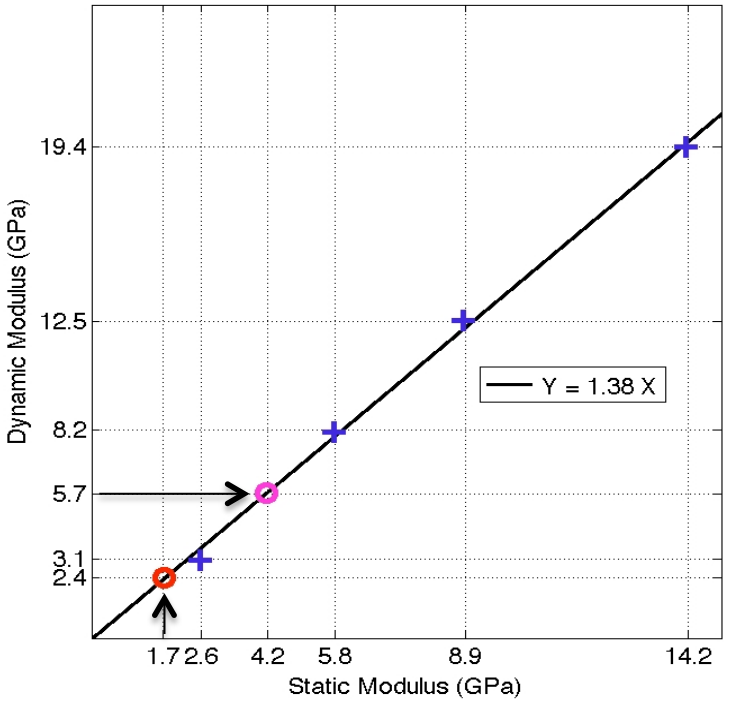

C11

C33

C66

C55

C12

C13

Elastostatics determine: C33,
C13,C11,C12,C66 (but not C55)

Ultrasonics determine:
C33,C12,C55,C66 (but not C13)

Doubly determined parameters are proportional: Dynamic=1.38 x Static

Singly determined moduli can be predicted by rescaling. ?!?

Moduli	C11	C13	C33	C55	C66	C12
Ultrasonics	19.4	**2.4**	12.5	5.7	8.2	3.1
Elastostatics	14.2	1.7	8.9	**4.2**	5.8	2.4
Dynamic Stat x 1.38	19.5	2.4	12.2	5.7	8.0	3.3
Static	14.1	1.7	9.1	4.1	5.9	2.3

Good news + Challenge

- Both ultrasonic and quasi-static measurements look like good measurements showing clear anisotropy
- Dynamic elastic moduli are systematically greater than the quasi-static moduli determined from small stress unloading cycles.
- There was a remarkably strong correlation between the static and dynamic moduli on this shale
- Consequently the two plug method enabled determination of *static* and *dynamic* values of all 5 TI parameters
- A research challenge is to document and understand the physics governing the difference between the static/dynamic modulus of shale
- I think that linear viscoelasticity is what we see here

Acknowledgements

Coauthors Dick Plumb, Greg Boitnott

Hunt Oil Dallas for permission to present this rock mechanics data

New England research for conducting the laboratory measurements and preliminary rock characterization